Renewable and Sustainable Energy Reviews 175 (2023) 113168

Contents lists available at ScienceDirect

Renewable and Sustainable Energy Reviews

journal homepage: www.elsevier.com/locate/rser

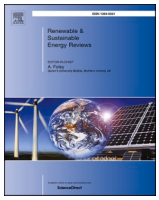

Techno-economic-environmental evaluation of aircraft propulsion electrification: Surrogate-based multi-mission optimal design approach

Jinning Zhang [a,b,c,*], Ioannis Roumeliotis [b], Xin Zhang [d,**], Argyrios Zolotas [c]

[a] Aerospace and Computational Group, School of Engineering, University of Leicester, Leicester, LE1 7RH, UK
[b] Centre for Propulsion and Thermal Power Engineering, School of Aerospace, Transport and Manufacturing, Cranfield University, Bedford, MK43 0AL, UK
[c] Centre for Autonomous and Cyber-physical Systems, School of Aerospace, Transport and Manufacturing, Cranfield University, Bedford, MK43 0AL, UK
[d] Department of Electrical and Electronic Engineering, Brunel University London, Uxbridge, UB8 3PH, UK

ARTICLE INFO

Keywords:
Aircraft propulsion electrification
Decarbonized aviation
Hybrid electric aircraft
Multi-mission optimal design
Energy management strategy
Fuel economy
Techno-economic evaluation
Environmental policy scenarios
Direct operating cost

ABSTRACT

Driven by the sustainability initiatives in the aviation sector, the emerging technologies of aircraft propulsion electrification have been identified as the promising approach to realize sustainable and decarbonized aviation. This study proposes a surrogate-based multi-mission optimal design approach for aircraft propulsion electrification, which innovatively incorporates realistic aviation operations into the electric aircraft design, with the aim of improving the overall aircraft fuel economy over multiple flight missions and conditions in practical scenarios. The proposed optimal design approach starts with the flight route data analysis to cluster the flight operational data using gaussian mixture model, so that a concise representation of flight mission profiles can be achieved. Then, an optimal orthogonal array-based Latin hypercubes are employed to generate sampling points of design variables for electrified aircraft propulsion. The mission analysis is performed with coupled propulsion-airframe integration in order to propose energy management strategy for mission-dependent aircraft performance. Consequently, fuel economy surrogate model is established via support vector machines to obtain the optimal design points of electrified aircraft propulsion. For assessing the viability of novel propulsion technologies, techno-economic evaluation is conducted using sensitivity analysis and breakeven electricity prices under a series of environmental regulatory policy scenarios.

1. Introduction

Projected by U.S. Energy Information Administration, a nearly 60% increase in global air travel seat miles and a 38% increase in energy use for aviation sector can be envisioned with corresponding CO_2 emissions projections of 209 million metric tons CO_2e by 2050 [1]. This will lead to the considerable negative environmental impacts due to the fossil-fuel dominated air travel. Thus, the civil aviation sector plays an increasingly significant role in transport sustainability with regard to environmental, economic, and social dimensions. In order to decarbonize the traditionally carbon-intensive aviation sector, electrified aircraft propulsion (EAP) have been identified and emerged as a promising technology, with advantages of on-board generating, distributing, and utilising electric power to eliminate direct combustion emissions in flight, as well as to improve the vehicle efficiency and performance [2]. In addition, the indirect CO_2 emissions from on-board electricity can be further alleviated on the ground energy infrastructure with the integration of renewable and sustainable energy sources, such as solar, wind and hydrogen [3]. The EAP architectures are generally classified as all-electric, hybrid-electric, and turboelectric. The potential benefits of block fuel burn reduction and CO_2 emissions reduction are significantly dependent on EAP configuration, electric component performance and flight missions [4]. For EAP, weight is a critical concern since the aircraft needs to account for the additional weight of batteries, electric machines, power electronics and follow-on structural growth [5]. Particularly, as an alternative energy source, battery demonstrates relatively low energy density comparing to the traditional jet fuel. As a result, the on-board batteries will significantly increase the weight of the EAP systems leading to drag penalty. Unlike the jet fuel, batteries will not lose mass along with the flight missions, this side effect of drag penalty will be further enlarged in long range missions. Thus, all-electric configuration of EAP is only capable of powering vertical take-off and landing aircraft, commuter aircraft, rotorcraft which only carry a few

* Corresponding author. Aerospace and Computational Group, School of Engineering, University of Leicester, Leicester, LE1 7RH, UK.
** Corresponding author.
E-mail addresses: jz388@leicester.ac.uk (J. Zhang), xin.sam.zhang@gmail.com (X. Zhang).

https://doi.org/10.1016/j.rser.2023.113168
Received 31 May 2022; Received in revised form 29 November 2022; Accepted 4 January 2023
Available online 10 January 2023

Nomenclature

Abbreviations

ANN	Artificial Neural Network
BAU	Business As Usual
BET	Baseline Environmental Taxation
BIC	Bayesian Information Criterion
DC	Data Centroids
DOC	Direct Operating Cost
DOE	Design of Experiment
EAP	Electrified Aircraft Propulsion
EEA	Exceptional Environmental Awareness
EM	Expectation-Maximization
EMS	Energy Management Strategy
FC	Flight cycles
FH	Flight hours
GA	Genetic Algorithm
GMM	Gaussian Mixture Model
HEA	Hybrid Electric Aircraft
HEPS	Hybrid Electric Propulsion System
MAE	Mean Absolute Error
MIPH	Mechanically Integrated Parallel Hybrid
MTOW	Maximum Take-Off Weight
NSGA	Non-dominated Sorting Genetic Algorithm
OA	Orthogonal Array
PEA	Progressive Environmental Awareness
PY	Per Year
RMSE	Root Mean Square Error
R-Squared	Coefficient of determination
SOC	State of Charge
SVMs	Support Vector Machines

Units

hrs	Hours
hp/lb	Horsepower per pound
K	Kelvin, the primary unit of temperature
km	Kilometre
kg	Kilogram
kPa	Kilopascal
kWh	Kilowatt hour
m	Meter
m^2	Square meters
m/s	Meter per second
MW	Megawatt
MWh	Megawatt hour
$	Dollar
Wh/kg	Watt-hour per kilogram

Symbols

$C_{Acquisition,FC}$	Acquisition cost per flight cycle
$C_{Acquisition,FH}$	Acquisition cost per flight hour
$C_{Aircraft}$	Acquisition price of aircraft
$C_{Aircraft,spares}$	The cost of aircraft spares
$C_{Battery}$	Acquisition price of battery
$C_{Battery,FC}$	Battery replacement cost per flight cycle
$C_{Breakeven,electricity}$	Breakeven electricity price
$C_{Capital\ Investment}$	Capital investment cost
$C_{carbontax}$	Carbon tax
$C_{Depreciation,PY}$	Depreciation cost per year
$C_{electricity}$	Price of electricity
$C_{Engines}$	Acquisition price of engine per unit
$C_{Engine/Airframe,FC}$	Engine and airframe maintenance cost per flight cycle
$C_{Energy,FC}$	Energy cost per flight cycle
$C_{Emissions,FC}$	Emission costs per flight cycle
C_{fuel}	Price of fuel
$C_{Motor/Inverter}$	Acquisition price of motor and inverter
$C_{\mathrm{Propulsion}}$	Acquisition price of propulsion
$C_{Propulsion,spares}$	The cost of propulsion spares
$C_{Insurance,PY}$	Yearly insurance cost
$C_{Interest,PY}$	Yearly interest cost
CN	Low-pressure shaft non-dimensional rotational speed
D	Aerodynamic forces of drag
$E_{bat,discharged}$	Battery capacity discharged during the flight
$E_{Design\_Battery}$	Battery energy storage capacity
$EICO_2f$	CO_2 emission indices for aviation fuel (Jet A)
$EICO_2e$	CO_2 intensity of electricity generation in UK
$EINOx$	NOx emission indices
$f_{Engine/Airframe,FH}$	Engine and airframe maintenance cost per flight hour
$f_{Battery,FH}$	Battery replacement cost per flight hour
F_N	Net thrust demand
g	Constant acceleration of gravity
h	Flight altitude
$h_{annul\ utilization}$	Annual utilization in terms of flight hours
Hp_{LPT}	Degree of hybridization of power on low pressure shaft
J_{CO_2}	Mission-dependent CO_2 emission
J_{NOx}	Mission-dependent NOx emission
L	Aerodynamic forces of lift
$P3$	Burner inlet pressure
P_{ontake}	Power on-take on low pressure shaft
P_{Design_Motor}	Motor power capacity
p_m	Gaussian density function for the m-th component
$P(\mathbf{x}\|\Theta)$	Gaussian mixture model specified by the set of parameters Θ
T	Aerodynamic forces of thrust
$T3$	Burner inlet temperature
$T4$	Turbine entry temperature
TF	Technology factor to adapt the NOx emission correlation
V	Aircraft velocity relative to the ground
W	Aircraft weight
W_f	Mission block fuel burn
$\dot{W}_f$	Engine fuel flow rate
ΔW_f	The reduced block fuel burn
$\mathbf{x}$	The flight route dataset
Y_{Life}	Aircraft operational life
z_m^i	The posterior probability of the m-th component in Gaussian Mixture
α	Angle of attack
α_m	The weight of the m-th component in Gaussian Mixture
ψ	Yaw heading angle
γ	Pitch/flight path angle
μ	Roll bank angle
μ_m	The mean vector of the m-th component in Gaussian Mixture
Σ_m	The covariance matrix of the m-th component in Gaussian Mixture
θ_m	The set of parameters for the m-th component in Gaussian Mixture
Θ	The set of parameters for Gaussian mixture
$\eta_{Bat\_charging}$	Battery charging efficiency
η_{trans}	Electricity transmission and distribution efficiency

passengers for general aviation [6]. However, by scaling up to an Airbus A320 or Boeing 737-sized aircraft, the perspective battery energy density requirements is significantly higher than any state-of-the-art Li-ion chemical capacities [6]. Thus, hybrid electric propulsion systems (HEPS) are proposed as a feasible solution for larger commercial aircrafts with long-haul flight ranges [7]. The HEPS exploits the electric power from batteries to power the motors, in combination with the low carbon alternative fuels to further deliver propulsion thrust. The HEPS is implemented as either a complementary or an alternative to conventional gas turbines [8]. The HEPS approach incorporates the electric machines within the gas turbine housing, which minimizes the alteration of gas turbine mechanical parts. This configuration has been commonly identified as the economic short-to medium-term solutions for aviation electrification.

Regarding the applications of EAPs, the key issue is to implement the integrated solutions for novel propulsion electrification technologies with the airframe. Traditional aircraft sizing involves a large number of iterations and the multidisciplinary analysis of aerodynamics, airframe, weight, manoeuvres, and fuel-based propulsion systems. The process aims to balance the thrust and drag within the top-level aircraft operational and performance constraints. For EAPs, the sizing procedure should be revised to include electric powertrain and dual energy sources, so that the new operating characteristics of electric/HEPS can be captured. Some studies have investigated the preliminary sizing and multidisciplinary optimization of aircraft propulsion electrification. In Ref. [9], Bocii et al. proposed an optimal design approach to investigate the trade-off between energy storage system sizing and the fuel mass for a series hybrid electric configuration of aircraft by using differential evolution algorithm. The powertrain sizing for hybrid electric rotorcrafts was proposed in Ref. [10], where the feasibility and potentiality of the hybridization schemes were investigated. Besides, Sliwinski et al. proposed a retrofit design method for hybrid electric unmanned aircraft in Ref. [11] to improve endurance or range. In Ref. [12], a hybrid electric aircraft (HEA) conceptual design procedure with power management strategy was investigated with two novel contributions: looping for power-split factor in take-off and climb phases as well as re-designing the gas turbine for cruise conditions. Decerio et al. applied numerical optimization to the conceptual design of regional aircrafts with parallel hybrid electric configurations to quantify the energy efficiency improvements [13]. Two sizing methods of hybrid electric aircraft proposed FH Aachen and TU Delft were compared and cross-validated in Ref. [14]. However, these previous studies only considered single design mission profile.

In practical scenarios, commercial aircrafts are expected to operate optimally in the actual flight missions which can be significantly different from the initial design mission. In addition, the significant increase in air traffic demand has imposed major impacts on aircraft operations. These integrated impacts between the increasing complexity of EAP systems operation and air traffic management requires multi-mission adaption in aircraft design. To address this challenge, this research work will innovatively integrate aircraft operational data into the design procedure by using multi-mission aircraft design optimization method, so that practical aviation operations can be incorporated into the aircraft design to improve the overall performance for multiple flight missions and conditions. The impact of aircraft design reference mission on fuel efficiency was investigated in Ref. [15], where a joint optimization approach of aircraft design and operations were proposed to improve fuel efficiency throughout the operational life of an aircraft. A multi-mission performance optimization approach was proposed for hybrid-electric unmanned aerial vehicles (UAVs) in Ref. [16], where the proposed methodology was applied by considering two specific missions: maximum endurance mission and a fixed range of 600 nmi with all-electric loiter segment. Similarly, a robust multi-mission design strategy was studied using non-dominated sorting genetic algorithm (NSGA) with a radial basis artificial neural network for aircraft conceptual design with specified short-range and long-range missions [17]. However, the specified design missions were user-defined and highly empirical. In order to improve the specified design missions, a multi-mission multi-objective optimization method for commercial aircraft conceptual design was proposed using NSGA II in Ref. [18]. This optimization method compared the difference between exclusively considering metrics of interest from one design mission and that of multiple missions, and further investigated the impact of weightings on optimization results. Particularly, this study considered three types of off-design missions: payload-range envelope, sample grid and user-defined missions. In Refs. [19,20], a robust aircraft design approach was proposed to avoid severe performance degradation at off-design conditions by considering hundreds of missions within the operational flight envelope. Herein [21], a payload-range space grid was created where the midpoints of all nonempty grid cells were selected as representative flight missions with the corresponding weights. Besides, a multidisciplinary optimization method for aircraft sizing was developed based on density-based spatial clustering algorithms. This method was used to integrate aircraft operational data from the initial design process to model realistic aircraft operations [22]. From the previous research work, the sample grid method with weighting factors can cover typical and representative missions, but this will lead to an excessive number of off-design mission evaluations. As a result, the design and operation of EAP over a range of propulsion system designs with series of missions are complex and computationally expensive. In order to improve the design efficiency of EAP systems, this study will propose a multi-mission optimal design so that the operational data can be integrated into the conceptual design procedure. The multi-mission design approach will be developed based on data clustering algorithms, with an important application to comprehensively analyse the tradeoff between the optimization accuracy, design robustness and computation efficiency of the EAP design and operation.

The economic viability and environmental impacts are essential for development of novel EAP technologies, with particular emphasis at the early and feasibility stages of such development [23]. In the aviation sector, fuel remains a major portion of operating costs which normally accounts for 40%. Thus, the fluctuations in fuel price are closely linked with an airline's profitability [24]. Therefore, the techno-economic analysis can be utilised in polices decisions, such as environment regulatory policies and incentives, to direct the aviation industry towards sustainable propulsion solutions. Previous studies have investigated the techno-environmental-economic analysis for aircraft propulsion electrification. Schäfer et al. exploited the economic and environmental benefits of all-electric aircrafts, which envisioned that all-electric aircraft fleet with a range of 600 nautical miles can substitute 15% of commercial aircraft fuel use and reduce 40% global landing and take-off NOx emissions. To achieve cost-effectiveness of electrified aircraft relative to jet engine aircraft, fuel prices was expected to be increased as well as end-use electricity prices required to be reduced accordingly with lower battery costs [25]. Besides, the environmental assessment of hybrid-electric propulsion in conceptual design was conducted from the perspectives of aircraft life cycle in Ref. [26]. In Ref. [27], potential benefits of operating costs reduction were investigated for a general aviation of CS-23 aircraft with the consideration of propulsion-airframe integration. Furthermore, technical and environmental assessment of all-electric 180-passenger commercial aircraft was performed in Ref. [28], which investigated the impacts of significant aircraft weight and performance penalties for each battery specific energy assumption case. The economic evaluation was conducted for turboelectric configuration in Ref. [29], which compared the recurring and cash operating costs of conventional aircraft and electrified propulsion derivatives. In Ref. [30], the environmental life cycle associated with direct operating costs were evaluated for a conventional A320 single-aisle aircraft and its hybrid electric derivatives. For lifecycle analysis, Wehrspohn et al. provided insights into the HEA performance over the entire lifecycle from economic and environmental perspectives for hydrogen powered HEA and the conventional fuel powered counterpart [31]. In Ref. [32],

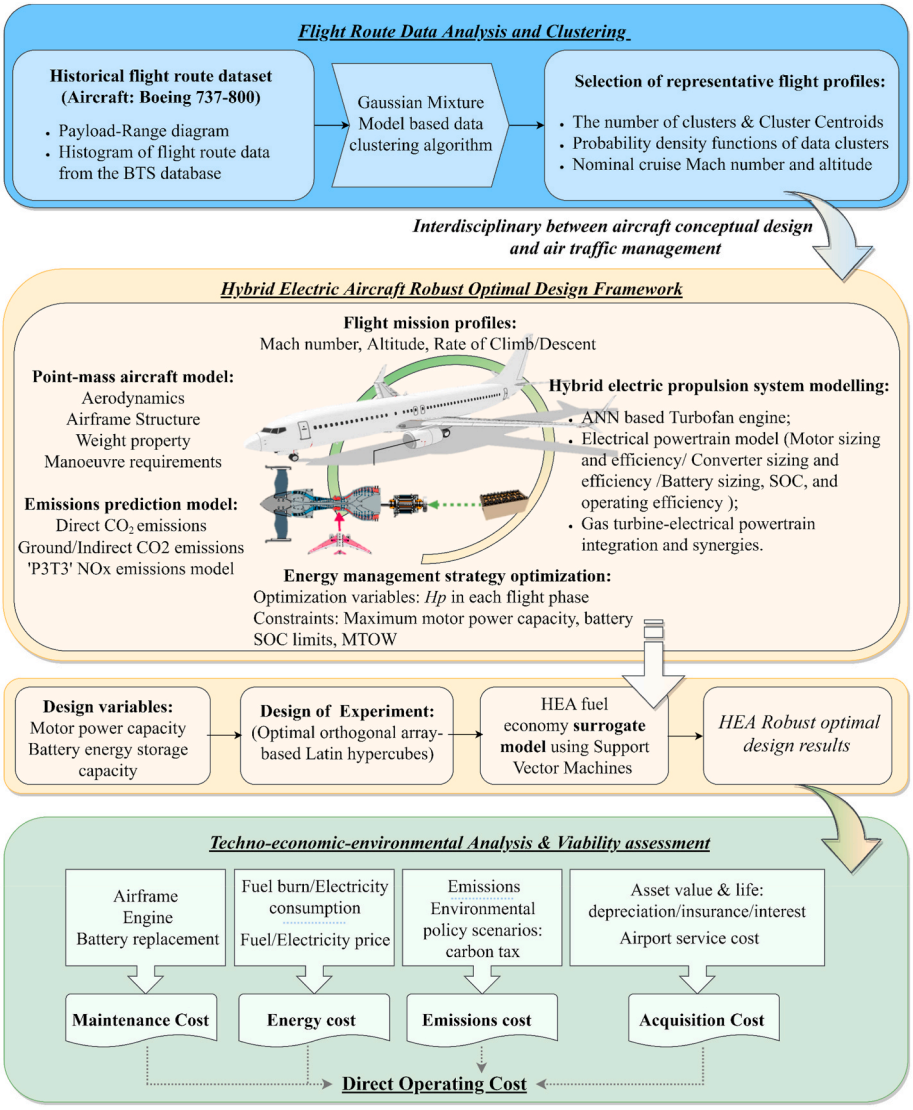

Fig. 1. Framework of HEA robust optimal design and techno-economic-environmental analysis.

the cost estimation method was proposed for HEA, which discussed the differences between conventional and HEA designs with particular impacts of HEPS on operating costs. In Ref. [33], the figures of merits, emissions, and operating costs were incorporated in the objective function for HEA design, which offered a detailed and transparent assessment in the initial design stages. The cost effectiveness of HEA versus conventional aircraft is critically dependent on the cost of batteries, electric machines, power electronics, and the relative costs of end-use electricity versus jet fuel. However, with advances in battery technologies and increasing development in production scale, the costs of electric components are expected to reduce significantly. Thus, the cost estimation of EAP is highly uncertain due to the uncertain development trend of these technologies. Therefore, sensitivity analysis of maintenance and acquisition costs, as well as breakeven electricity price versus jet fuel price, are essential to study the economic viability of EAP technologies in this research work.

In this research work, a multi-mission based optimal design approach for aircraft propulsion electrification is proposed. Then, the techno-environmental-economic assessment is conducted to investigate the prerequisites of aircraft propulsion electrification to achieve cost-effectiveness. The novel contributions of this research work are provided as follows to support aircraft propulsion electrification design and operation, which will further aid the environmental regulatory policy scenarios.

- A novel multi-mission based optimal design approach is proposed for aircraft propulsion electrification. The proposed method innovatively incorporates realistic aviation operations into the aircraft conceptual design phase, in order to optimize the aircraft fuel economy over multiple flight missions and conditions.
- The HEA mission analysis framework with genetic algorithm-based optimal EMS is developed in this study. The framework involves a multidisciplinary analysis of aerodynamics, airframe, weight, manoeuvres and propulsion. The propulsion model considers the closely coupled synergies of gas turbine and electric powertrain. On this basis, the fuel economy surrogate models are established for each flight route cluster, which can be incorporated to achieve multi-mission optimal design.
- The techno-environmental-economic evaluation method is developed for HEA, which accounts for a wide range of costs including fuel, electricity, emissions, maintenance and acquisition costs. The sensitivity and cost-effectiveness analysis of acquisition and maintenance cost, as well as breakeven electricity price are discussed in potential environmental regulatory policy scenarios.

The remaining of the paper is organized as follow: Section 2 consists

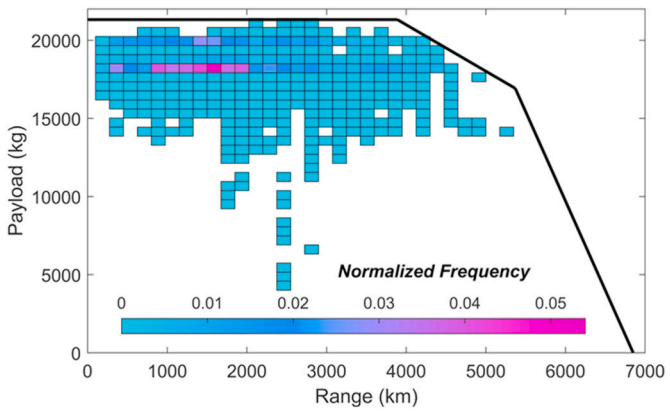

Fig. 2. Payload-Range diagram and Histogram of flights for Boeing 737–800 aircraft during the year of 2018 [34,35].

of problem formulation and method. In each sub-section, the historical flight route data analysis and clustering is conducted in Section 2.1 in order to select the representative flight mission profiles. In Section 2.2, hybrid electric aircraft modelling and mission analysis are introduced, including the propulsion system modelling the integration of novel propulsion technologies with airframe, and the mission analysis method with EMS optimization. Then, in Section 2.3, the surrogate-based optimal design approach for aircraft propulsion electrification is proposed, which comprises major steps of design of experiment, fuel economy surrogate model generation, and fuel economy optimization. Section 3proposes the environmental and economic evaluation models. Section 4 presents the results of the case studies and the related sensitivity analysis. Finally, Section 5 draws conclusions of this research.

2. Problem formulation and methods

The proposed framework of this study for HEA modelling, optimal design and operation, and techno-economic-environmental analysis for viability assessment is presented in Fig. 1.

2.1. Flight route data analysis and clustering

The representative flight mission profile is selected based on historical flight route data which reflects the variability in flight operations. The historical flight route of Boeing 737–800 is obtained in Bureau of Transportation Statistics flight database [34] with payload-range diagram [35] as Fig. 2.

Based on the data collection, Gaussian Mixture Model (GMM) is used for data clustering so that grouping of flight operational data can be identified from a large historical flight route of Boeing 737–800 dataset. The data collection and clustering are able to produce a concise representation of flight mission profiles. GMM is one of the commonly used and statistically mature methods for clustering. GMM is a probabilistic model which assumes all the data points are generated from a mixture of a finite number of clusters. These clusters are represented by gaussian distributions with unknown parameters [36]. The clustering process for fitting mixture-of-Gaussian models is usually implemented by expectation-maximization (EM) algorithms [37].

A finite mixture model $P(\mathbf{x}|\Theta)$ is the weighted sum of the components $p(\mathbf{x}|\theta_m)$ as equation (1) [37]:

$$P(\mathbf{x}|\Theta) = \sum_{m=1}^{M} \alpha_m p_m(\mathbf{x}|\theta_m)$$
$$s.t.\ \ \Theta = \{\alpha_1, \alpha_2, \cdots, \alpha_M, \theta_1, \theta_2, \cdots, \theta_M\} \quad (1)$$
$$\sum_{m=1}^{M} \alpha_m = 1$$

Where the gaussian mixture is specified by the set of parameters $\Theta = \{\alpha_1, \alpha_2, \cdots, \alpha_M, \theta_1, \theta_2, \cdots, \theta_M\}$, α_m is the weight of each component, eachp_m is a gaussian density function parameterized by $\theta_m = \{\mu_m, \Sigma_m\}$, μ_m, Σ_m are mean and covariance respectively.

In order to estimate Θ, the log likelihood function is defined with a set of data points $\mathbf{X} = (\mathbf{x}^1, \cdots \mathbf{x}^N)$ as equation (2), the expectation step and maximization step of EM algorithm are alternately applied until $\mathscr{L}(\Theta)$ converges to a local optimum [37].

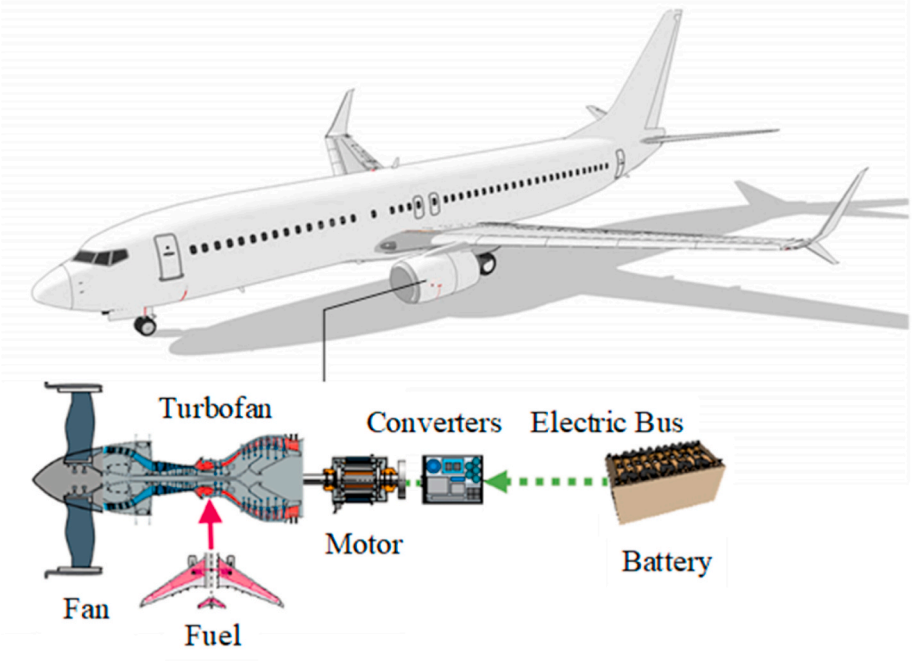

Fig. 3. The architecture of MIPH [38].

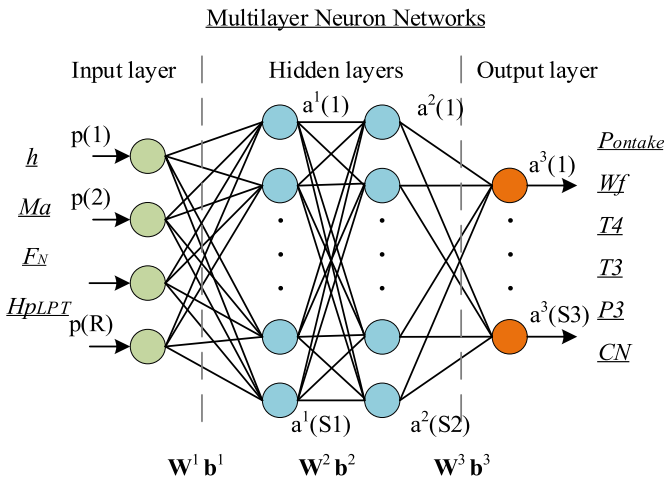

Fig. 4. ANN-based turbofan engine state-state performance model [39].

Table 1
Technology improvements projections of electric components (relative to the year 2015) [40].

	Unit	30-year estimate (2045)
Electric machine energy density	hp/lb	16
Electric machine efficiency	percent	97%
Power electronics energy density	hp/lb	15
Power electronics efficiency	percent	99%
Battery specific energy	Wh/kg	1400

Table 2
Aircraft model parameters and flight mission profile [39].

Aircraft model parameters	
Aircraft	Boeing 737-800
Category	Regional jets
Maximum take-off weight	79015.80 kg
Operating empty weight	41140.00 kg
Wing area	124.86 m^2
Wingspan	34.32 m
Aspect ratio	10.18
Nominal cruise Mach number	0.785
Nominal cruise altitude	10668.00 m
Climb rate	6.0/6.0/3.0 m/s
Descent rate	4.5/5.0/5.0/5.0/3.0 m/s

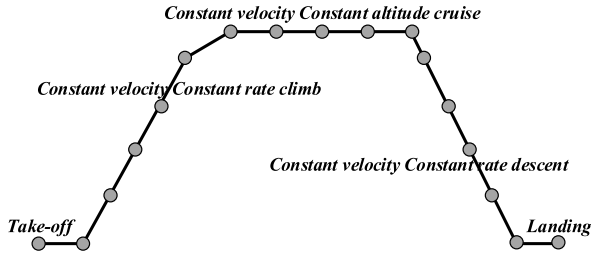

Fig. 5. Flight mission profile definition [39].

$$\mathscr{L}(\Theta) = \log p(\mathscr{X}|\Theta) = \log \prod_{i=1}^{N} p(\mathbf{x}^i|\Theta) = \sum_{i=1}^{N} \log\left(\sum_{m=1}^{M} \alpha_m p_m(\mathbf{x}^i|\theta_m)\right) \tag{2}$$

In expectation step, the dataset X is assumed to be incomplete and the complete dataset $\mathscr{Y} = (\mathscr{X}, \mathscr{Z})$ is determined by estimating the set of variables $\mathscr{Z} = \{\mathbf{z}_1, \mathbf{z}_2, \ldots \mathbf{z}_M\}$, where z_m is an N-dimensional vector $[z_m^1, z_m^2, \ldots, z_m^N]^T$. The log likelihood of the complete dataset $\mathscr{Y}$ is presented in Equation (3) [37]:

$$\log p(\mathscr{Y}|\Theta) = \sum_{i=1}^{N}\sum_{m=1}^{M} z_m^i \log\left[\alpha_m p(\mathbf{x}^i|\theta_m)\right] \tag{3}$$

$$z_m^i = P(m|\mathbf{x}^i, \Theta^t) = \frac{\alpha_m^t p(\mathbf{x}^i|\theta_m^t)}{\sum_{l=1}^{M} \alpha_l^t p(\mathbf{x}^i|\theta_l^t)}$$

Where z_m^i is the posterior probability and Θ^t is the parameter estimate obtained after t iterations.

In maximization step, the parameters Θ^{t+1} are determined based on the posterior probability z_m^i, which refer to $\alpha_m^{t+1}, \mu_m^{t+1}, \Sigma_m^{t+1}$ for each component m in GMM as Equation (4).

$$\alpha_m^{t+1} = \frac{1}{N}\sum_{i=1}^{N} z_m^i,$$

$$\mu_m^{t+1} = \frac{\sum_{i=1}^{N} z_m^i \mathbf{x}_i}{\sum_{i=1}^{N} z_m^i}, \tag{4}$$

$$\Sigma_m^{t+1} = \frac{\sum_{i=1}^{N} z_m^i (\mathbf{x}_i - \mu_m^{t+1})(\mathbf{x}_i - \mu_m^{t+1})^T}{\sum_{i=1}^{N} z_m^i}$$

2.2. Hybrid electric aircraft modelling and mission analysis

In this study, HEPS is modelling as mechanically integrated parallel hybrid propulsion configuration (MIPH). As shown in Fig. 3, in MIPH configuration, motor is mounted on the low-pressure shaft of turbofan engine, and then to drive the ducted fan where the electrical power is directly fed to the drive train of the propulsion device. The case studies will utilise Boeing 737–800 with dual hybridized CFM56 turbofan engines.

The turbofan engine steady-state performance model is developed based on artificial neural network (ANN) with back-propagation algorithm [39]. As shown in Fig. 4, the ANN-based turbofan engine performance model consists of an input layer, two hidden layers and an output layer as the neuron network structure of 4–10-10-6. The input layer has the elements of flight altitude (h), flight Mach number (Ma), net thrust demand (F_N), and degree of hybridization of power on low pressure shaft (Hp_{LPT}). The output layer has the elements of power on-take on low pressure shaft (P_{ontake}), fuel flow rate ($\dot{W}_f$), turbine entry temperature ($T4$), burner inlet temperature ($T3$), burner inlet pressure ($P3$), and low-pressure shaft non-dimensional rotational speed (CN). These turbofan engine operating characteristics will be used to estimate fuel economy, energy consumption and emissions performance.

The electrical powertrain model is established as [39]. Firstly, a rubber motor efficiency model is established for a hypothetical motor which has not been built or designed. Design parameters of peak efficiency, rotational speed, and torque at peak efficiency are specified. An equivalent circuit model is used for battery energy storage modelling to estimate battery operating efficiency and state of charge (SOC). The power electronics is assumed as constant efficiency. The technology level projections of electric components are listed in Table 1 [40].

A point-mass aircraft model is used for aircraft motion simulation as shown in equation (5). The basic aircraft model parameters and flight mission profile are listed in Table 2 and Fig. 5.

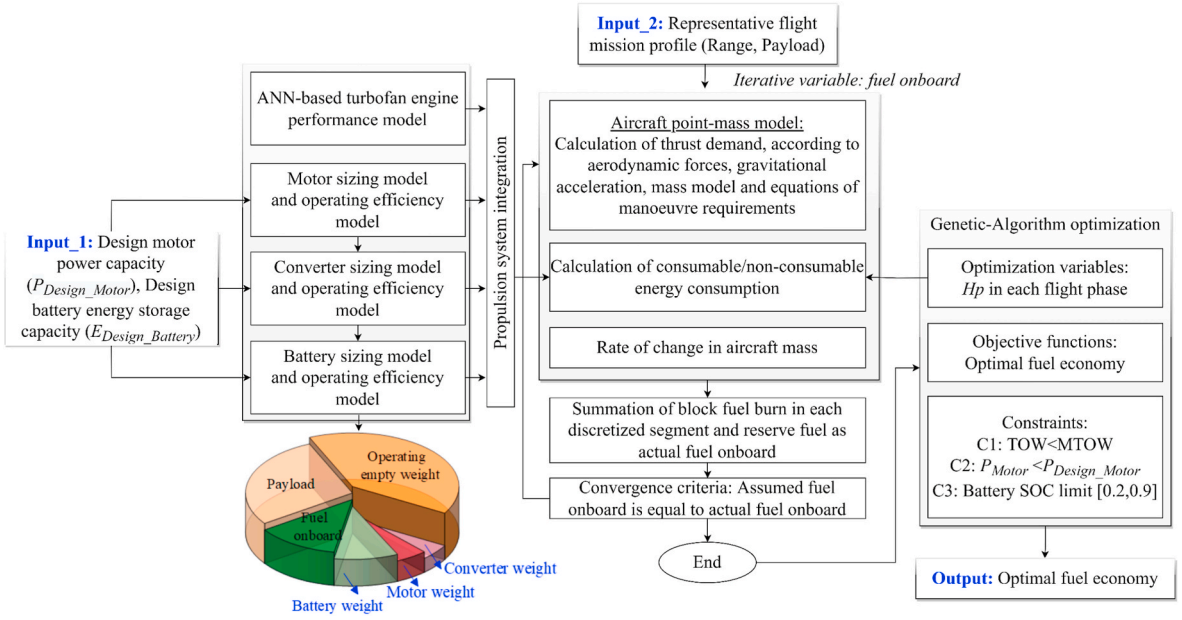

Fig. 6. HEA mission analysis with GA-based optimal EMS [38].

$$\frac{d}{dt}\begin{bmatrix}\dot{x}\\ \dot{y}\\ \dot{h}\\ \dot{V}\\ \dot{\psi}\\ \dot{\gamma}\\ \dot{W}\end{bmatrix}=\begin{bmatrix}V\cos(\psi)\cos(\gamma)\\ V\sin(\psi)\cos(\gamma)\\ V\sin(\gamma)\\ \frac{g}{W}[T\cos(\alpha)-D-W\sin(\gamma)]\\ \frac{g}{WV\cos(\gamma)}[T\sin(\alpha)+L]\sin(\mu)\\ \frac{g}{WV}[(T\sin(\alpha)+L)\cos(\mu)-W\cos(\gamma)]\\ -\dot{W}_f\end{bmatrix} \tag{5}$$

Where *x, y, h* represent the position of aircraft in ground axis coordinated system, *V* is the aircraft velocity relative to the ground, ψ, γ, μ denote yaw heading angle, pitch/flight path angle and roll bank angle respectively, *W* is the weight of aircraft, α is the angle of attack, $\dot{W}_f$ is the engine fuel flow rate, *T, D, L* are the aerodynamic forces of thrust, drag and lift respectively, *g* is the constant acceleration of gravity.

HEA mission analysis is an iterative process to balance the thrust and drag. HEA mission analysis converges to a solution of energy balance (required energy versus energy carried onboard) within the set operational and performance constraints defined by the top-level requirements, such as payload, range, rate of climb/descent, take-off field length, and cruise point airspeed. The mission analysis model has been adapted with optimal energy management strategy (EMS) for HEA design [38] which will consider the fully coupled aerodynamics-propulsion effects, as presented in Fig. 6.

Firstly, the input design variables are identified as motor power capacity (P_{Design_Motor}) and battery energy storage capacity ($E_{Design\_Battery}$). The sizing and operating efficiency models of electric powertrain are established accordingly. Then, the HEPS modelling is achieved by integrating ANN-based gas turbine surrogate model and power flow-based electric powertrain model.

The specified flight mission profile is discretized into a series of segments. In each segment, based on energy-based approach, the amount of depleted variable weight fuel (consumable energy source) and the fixed weight battery (non-consumable energy source) are calculated based on Hp_{LPT}, flight conditions, HEPS modelling, and aircraft point-mass model. The calculation involves a multidisciplinary analysis of aerodynamics, airframe, weight, manoeuvres, and propulsion system characteristics of both fuel-based gas turbine and power-based electric powertrain [41]. The flight conditions, aircraft weight, battery SOC are updated segment by segment accordingly. The fuel depleted in each flight segment is summed up to obtain the total mission fuel consumption. The iterations are converged when the assumed fuel onboard is equal to actual mission fuel consumption.

For EMS optimization, the genetic algorithm (GA) is applied to obtain the optimal fuel economy. The Hp_{LPT} in each flight phase are taken as the optimization variables. The input of design variables (P_{Design_Motor} and $E_{Design\_Battery}$) are taken as constraints, where the motor operating power should be less than P_{Design_Motor}, and the battery SOC should be operated within [0.2, 0.9]. The fuel economy surrogate model is further developed based on HEA mission analysis process with EMS.

Fig. 1 illustrates the framework and associated procedure of multi-mission HEA robust optimal design in this research. The design variables for HEA optimization include motor power capacity (P_{Design_Motor}) and battery energy storage capacity ($E_{Design\_Battery}$). In an initial design of experiment (DOE) stage, optimal orthogonal array (OA)-based Latin hypercubes method is adopted to generate a set of non-collapsing sampling points for design variables of P_{Design_Motor} and $E_{Design\_Battery}$ [42].

With regards to each sampling point, mission analysis with optimal EMS is then performed to obtain the optimal fuel economy as shown in Fig. 6. The mission analysis is evaluated for a wide range of the representative flight mission profiles selected from flight data clustering, which will be used to obtain mission-dependent aircraft fuel economy. Based on the mission analysis, the HEA fuel economy surrogate model is established using a regression algorithm support vector machines (SVMs) [43–45]. SVMs can significantly reduce the computational complexity by considering the error approximation to the data as well as the generalization of the model to evaluate new dataset [46]. The regression learning problem is used to learn the input-output dependency $f(x)$ that minimizes the empirical risk usingε insensitivity loss function given as (6) [47],

Table 3
Potential environmental regulatory policy scenarios.

Scenario	Carbon tax ($/Metric Ton)
Business As Usual (BAU)	0
Baseline Environmental Taxation (BET)	50
Progressive Environmental Awareness (PEA)	100
Exceptional Environmental Awareness (EEA)	200

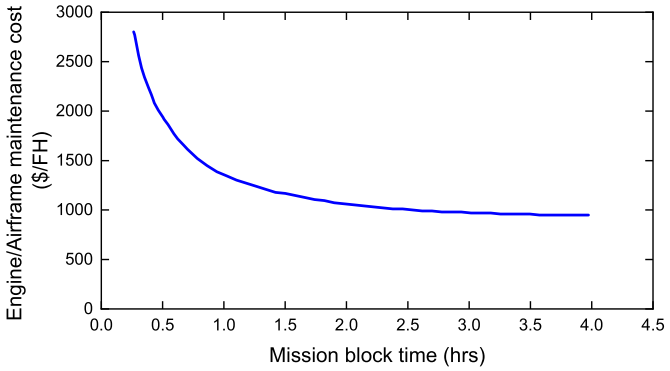

Fig. 7. Engine/airframe maintenance cost versus mission block time [52].

Table 4
The aircraft acquisition cost parameters [25,53].

Parameters	Value
Acquisition price of aircraft	80.8 US $ million
Acquisition price of engine per unit	8.4 US $ million
Acquisition price of battery	100 $/kWh
Acquisition price of motor and inverter	78$/kW
Annual utilization in terms of flight hours	3300 h
Annual utilization in terms of flight cycles	1700
Cost of airframe spares	10%
Cost of propulsion unit spares	30%
Aircraft operational life	20 years
Residual value of aircraft due to depreciation at end of life	10%
Interest on investment	5.5%
Insurance on investment	0.5%

$$R = \frac{1}{2}\|w\|^2 + C\sum_{i=1}^{N}|y_i - f(x_i)|_\varepsilon$$

$$s.t.\begin{cases} \forall n : y_n - f(x_n) \le \varepsilon + \xi_n \\ \forall n : f(x_n) - yn \le \varepsilon + \xi_n^* \\ \forall n : \xi_n \ge 0, \xi_n^* \ge 0 \end{cases} \quad (6)$$

Where the training dataset consists of n pairs $(x_1,y_1),(x_2,y_2),\ldots,(x_n,y_n)$, the inputs are multi-dimensional vectors and system responses y, $\|w\|$ is the weight vector norm, ε is the insensitivity zone, ξ_n andξ_n^* are slack variables, C is box constraint.

Herein, the nonlinear SVM regression model is adopted with a nonlinear, positive definite, gaussian radial basis function kernels as in equation (7) [47],

$$G(x_i,x_j) = \exp\left(-\left[\|x_i - x_j\|^2\right]/2\sigma^2\right) \quad (7)$$

The regression learning problem can be formulated as the maximization of a dual Lagrangian with nonnegative multipliers α_i, α_i^* for each observationx_i as in equation (8), which is used to obtain the coefficients of nonlinear SVM regression model [47],

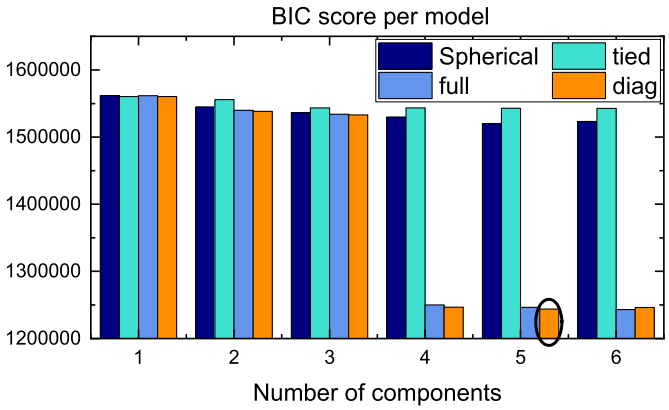

Fig. 8. BIC for the number of components and the covariance matrix structure.

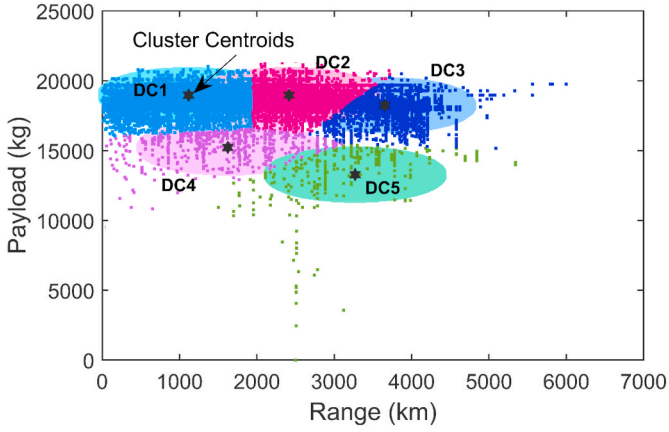

Fig. 9. Historical flight operational data clustering using GMM.

Table 5
Historical flight data cluster centroids and probability density.

	Unit	DC1	DC 2	DC 3	DC 4	DC 5
Range (Cluster centroids)	km	1117.07	2415.46	3652.69	1623.52	3270.25
Payload (Cluster centroids)	kg	18960.9	18962.7	18241.7	15224.1	13281.7
Probability density	–	0.5818	0.2855	0.1058	0.0153	0.0116

$$L(\alpha_i,\alpha_i^*) = -\frac{1}{2}\sum_{i=1}^{N}\sum_{j=1}^{N}(\alpha_i - \alpha_i^*)\left(\alpha_j - \alpha_j^*\right)G(x_i,x_j)$$

$$-\varepsilon\sum_{i=1}^{N}(\alpha_i + \alpha_i^*) + \sum_{i=1}^{N} y_i(\alpha_i - \alpha_i^*)$$

$$s.t.\begin{cases} \sum_{n=1}^{N}(\alpha_n - \alpha_n^*) = 0 \\ \forall n : 0 \le \alpha_n \le C \\ \forall n : 0 \le \alpha_n^* \le C \end{cases} \quad (8)$$

The optimal solution must satisfy the Karush-Kuhn-Tucker complementarity conditions as in equation (9):

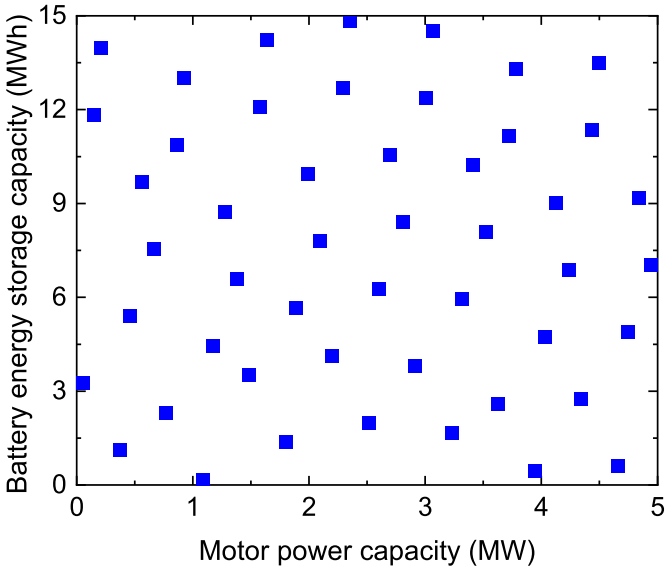

Fig. 10. Optimal OA-based Latin hypercubes sampling for design variables.

$$\begin{cases} \forall n : \alpha_n(\varepsilon + \xi_n - y_n + f(x_n)) = 0 \\ \forall n : \alpha_n^*(\varepsilon + \xi_n^* + y_n - f(x_n)) = 0 \\ \forall n : \xi_n(C - \alpha_n) = 0 \\ \forall n : \xi_n^*(C - \alpha_n^*) = 0 \end{cases} \tag{9}$$

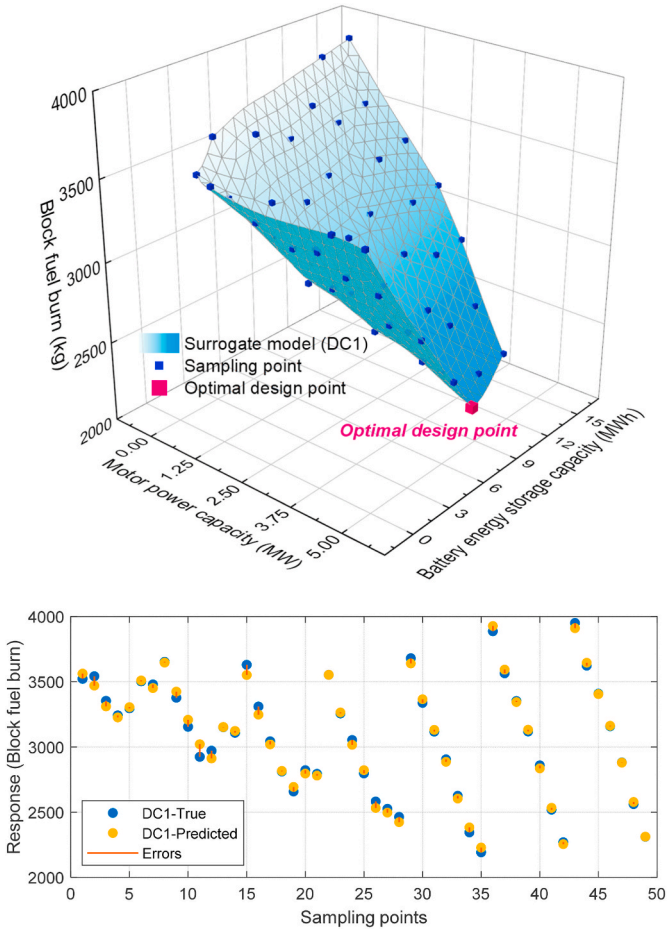

Fig. 11. Fuel economy surrogate model and error distribution for DC1.

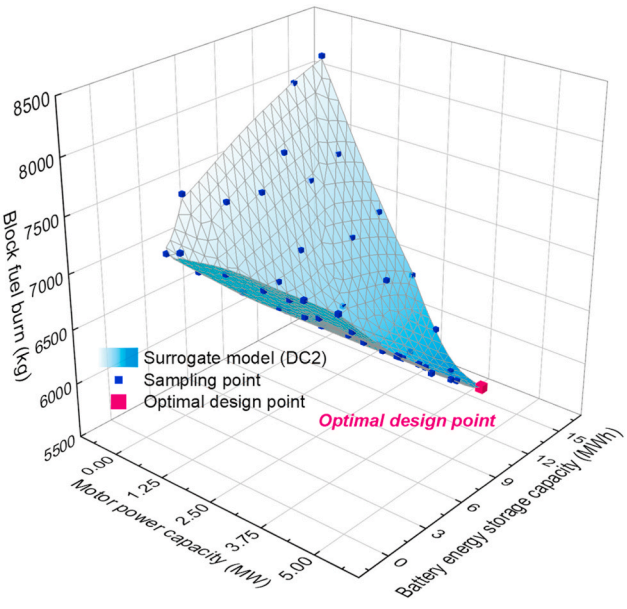

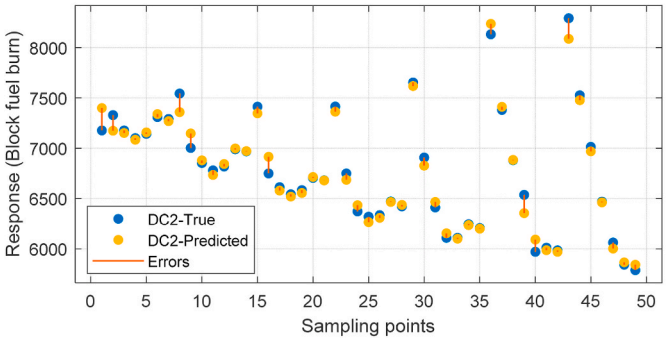

Fig. 12. Fuel economy surrogate model and error distribution for DC2.

The best regression hyperplane can be obtained in equation (10) [47]:

$$f(x) = \sum_{n=1}^{N} (\alpha_n - \alpha_n^*) \cdot G(x_n, x) + b \tag{10}$$

The surrogated-based approach for HEA optimal design is formulated to obtain optimal fuel economy considering flight operational data. The proposed design framework is an effective approach to address the aircraft propulsion electrification optimal design challenges imposed by complex objective functions evaluations involving multidisciplinary analysis, hard constraints of MTOW, battery SOC operating limits and motor power capacity, and the computational burden. In this case, the optimization objective is formulated as equation (11) with mission-dependent fuel economy and probability density:

$$\left[P^*_{Design\_Motor}, E^*_{Design\_Battery}\right] = \operatorname{argmin}\left(\sum_{i=1}^{M}\left(w(i)\cdot\frac{W_f\left(R(i), p(i)\middle|P_{Design\_Motor}, E_{Design\_Battery}\right)}{R(i)\cdot p(i)}\right)\right) \tag{11}$$

Where M denotes the feasible space of a bounded domain in flight mission range and payload, $w(i)$ is probability density of flight mission profile distribution, $W_f(R(i), p(i)|P_{Design\_Motor}, E_{Design\_Battery})$ is mission-dependent performance metric of block fuel burn, which is exclusively determined by payload $p(i)$ and range $R(i)$ for a sized hybrid electric aircraft with P_{Design_Motor} and $E_{Design\_Battery}$. The ratio of the block fuel burn liberated during a flight W_f to the revenue work done $R(i)\cdot p(i)$ is

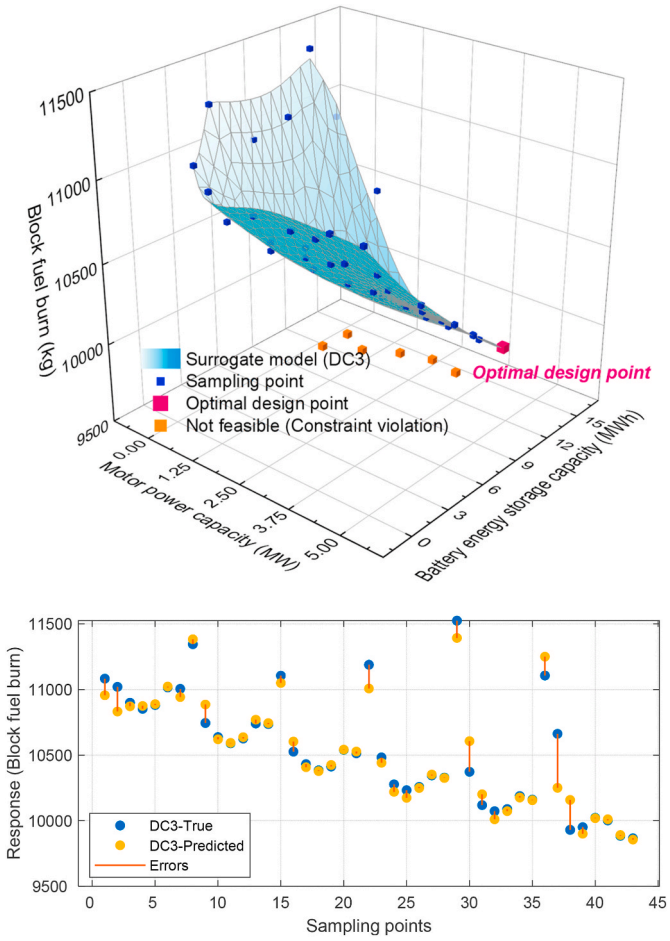

Fig. 13. Fuel economy surrogate model and error distribution for DC3.

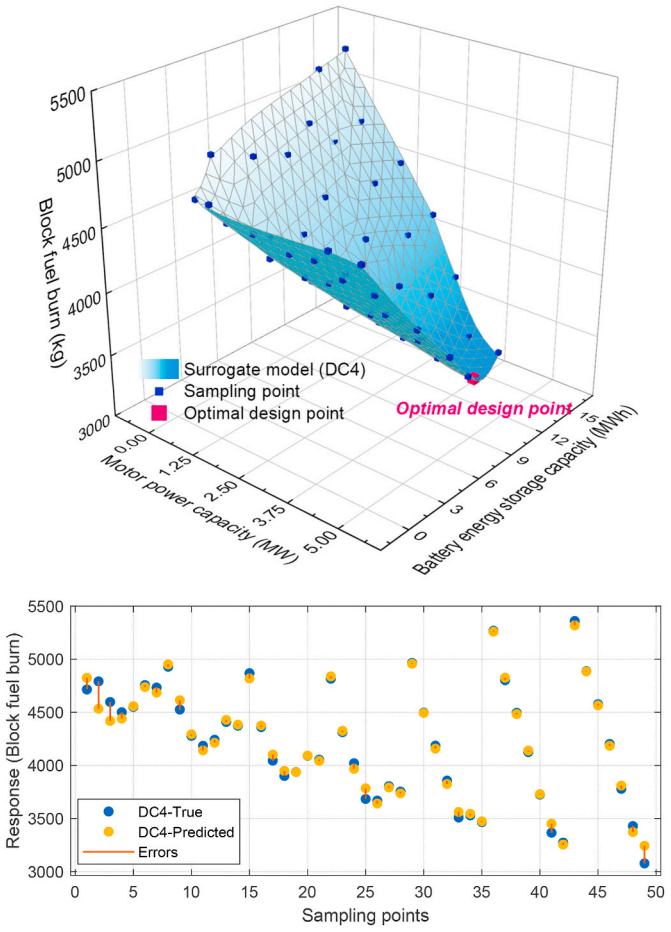

Fig. 14. Fuel economy surrogate model and error distribution for DC4.

employed as the key parameter to assess the fuel economy performance.

3. Environmental and economic evaluations

3.1. Environmental analysis

The emission prediction model is presented in this research by considering the direct combustion emissions of CO_2 and NOx emission as well as indirect CO_2 emission from the electricity used in the battery onboard.

The CO_2 emission from direct combustion is considered to be in equilibrium which is independent of HEA operational parameters. Thus, direct combustion CO_2 emission is modelled as proportional to block fuel burn and fuel composition. Particular, the CO_2 emission indices ($EICO_2f$) for aviation fuel (Jet A) of 3159 g CO_2/kg fuel is used to calculate the direct CO_2 emission. The indirect CO_2 emission is determined by the CO_2 intensity of electricity generation, battery charging efficiency, and associated energy infrastructure efficiency for the electricity production, transmission, and distribution [25]. The CO_2 intensity of electricity generation ($EICO_2e$) is considered as 130 g CO_2/kWh as an example in the UK [48]. In total, the mission-dependent CO_2 emission J_{CO_2} can be calculated in equation (12):

$$J_{CO_2} = EICO_2f \cdot W_f + EICO_2e \cdot \frac{E_{Design\_Battery} \cdot (SOC_{end} - SOC_{initial})}{\eta_{Bat\_charging} \cdot \eta_{trans}} \tag{12}$$

Where the battery charging efficiency $\eta_{Bat\_charging}$ is set at 95%, and electricity transmission and distribution efficiency η_{trans} is considered as 95% [25].

NOx emission is predicted using a semi-empirical correlations approach, *'P3T3'* method with aero engine internal gas path parameters at combustor diffuser inlet [49]. The NOx emission indices ($EINOx$) and mission-dependent NOx emission J_{NOx} are given in equations (13) and (14):

$$EINOx = \left(a + b \cdot e^{cT3}\right)\left(\frac{P3}{P3_{ref}}\right)^{d} \cdot e^{f(h_{SL}-h)} \cdot \left(\frac{\Delta T_{comb}}{\Delta T_{comb,ref}}\right)^{TF} \tag{13}$$

$$J_{NOx} = \int_{t}^{t_f} EINOx(t) \cdot \dot{W}_f(t)dt \tag{14}$$

Where default values for the constants and exponents suitable for a modern civil turbofan engine are $a = 8.4, b = 0.0209, c = 0.0082, d = 0.4, f = 19, TF = 0, P3_{ref} = 3000kPa, \Delta T_{comb,ref} = 300K, h_{SL} = 0.006344$ [49].

3.2. Economic analysis

Direct operating cost (DOC) is considered as the essential figure of merit for the economic viability in aircraft design studies. As shown in Fig. 1, the DOC per mission is generally composed of energy (fuel and electricity) cost, emissions cost, maintenance cost and acquisition cost respectively.

The energy cost is evaluated as a function of the aircraft mission performance which is dependent on the flight mission profile. The energy cost is derived from mission block fuel burn, electricity consumption, and the current fuel price (1157.10 $/Metric Ton) and electricity price (10.55 Cents/kWh). The fuel price for aviation jet fuel is specified by the International Air Transport Association jet fuel price monitor [50]. The electricity price for transportation sector is specified by U.S.

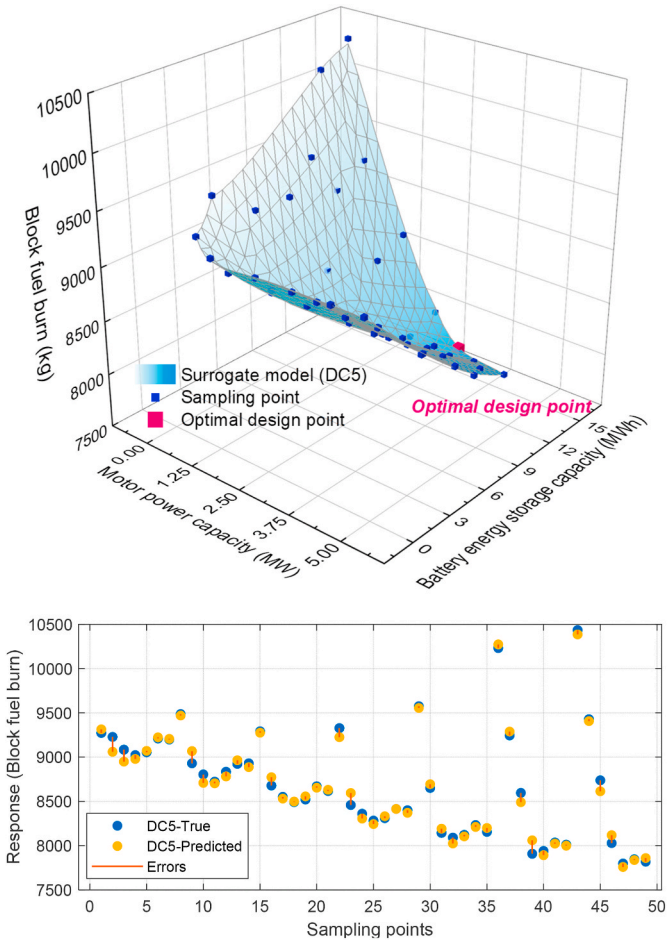

Fig. 15. Fuel economy surrogate model and error distribution for DC5.

Table 6
Fuel economy surrogate model regression validation.

	DC1	DC2	DC3	DC4	DC5
RMSE	34.89	79.65	103.31	63.60	65.93
R-Squared	0.99	0.98	0.94	0.99	0.99
MAE	27.45	55.17	61.41	40.10	50.18

Energy Information Administration [51].

Thus, the energy cost per flight cycle (FC) $C_{Energy,FC}$ is calculated as equation (15):

$$C_{Energy,FC} = C_{fuel} \cdot W_f + C_{electricity} \cdot E_{bat,discharged} \quad (15)$$

Where W_f is the mission block fuel burn during the flight, $E_{bat,discharged}$ is the battery capacity discharged during the flight.

The energy and emission costs are correlated, with both being a function of aircraft mission performance. The emission costs are estimated based on the carbon tax scenarios $C_{carbontax}$, and the amount of emissions W_{CO_2} as equation (16).

$$C_{Emissions,FC} = C_{carbontax} \cdot W_{CO_2} \quad (16)$$

The incentive policies on low-carbon electricity and carbon tax are essential for aviation electrification. Therefore, several carbon tax scenarios are selected to investigate the effects of environmental regulatory policies on emission costs as presented in Table 3 [52].

The maintenance cost considers airframe maintenance, engine maintenance and battery replacement cost. The aircraft is normally considered to have a certain average annual utilization in terms of flight

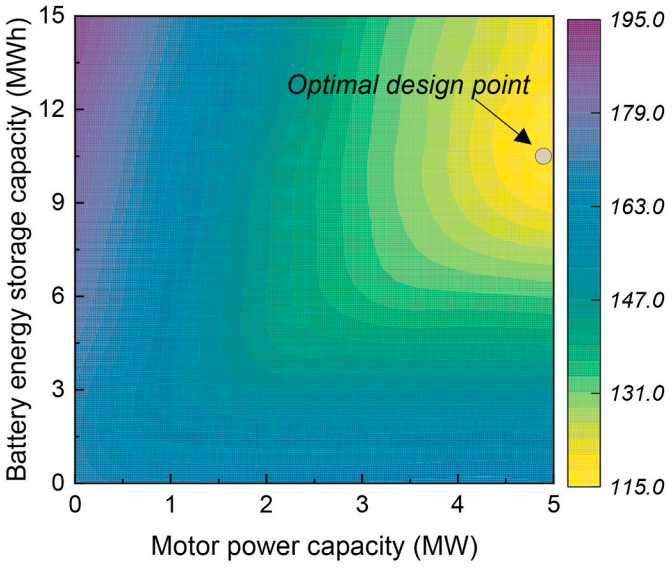

Fig. 16. Optimal design point of multi-mission fuel economy surrogate model.

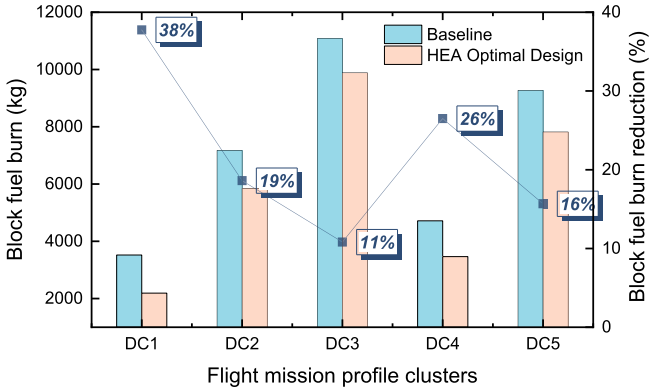

Fig. 17. Fuel economy benefits with multi-mission HEA optimal design.

cycles (FC) or flight hours (FH). Herein, for conventional single aisle aircraft such as Boeing 737–800 powered by dual CFM 56 turbofan engines, an annual utilization of 3300 flight hours or 1700 flight cycles is normally assumed [52]. The maintenance cost of engine and airframe per hour is estimated based on the public domain data of Boeing 737–800's direct maintenance costs [53], the periodicity of the maintenance routines, the assumed mission block time and the annual utilization of flight cycles and flight hours. The relationship between engine/airframe maintenance cost and the average mission block time is illustrated in Fig. 7 [52]. Herein, the maintenance cost of engine and airframe for the types of aircraft between conventional and HEPS are assumed to be equal. In addition, the impact of electrification on engine operational life is not considered in this research work.

Thus, the maintenance cost for engine and airframe per flight cycle $C_{Engine/Airframe,FC}$ is given as Equation (17):

$$C_{Engine/Airframe,FC} = f_{Engine/Airframe,FH}(t_{mission}) \cdot t_{mission} \quad (17)$$

Where $f_{Engine/Airframe,FH}$ is the engine/airframe maintenance cost per flight hour versus mission block time, $t_{mission}$ is the mission block time calculated from aircraft mission simulation.

Similarly to electric vehicles, battery maintenance for EAP is a major concern given the relatively frequent replacement or upgrade during the long lifespan of the aircraft. The battery aging and replacement costs after their end operational life of 5000 cycles is considered in the

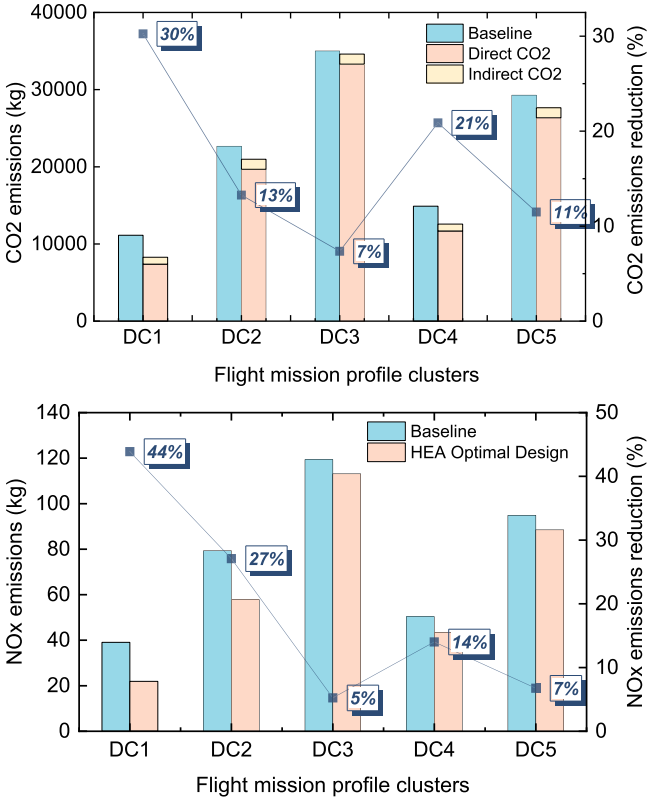

Fig. 18. Environmental analysis for CO_2 emissions and NOx emissions.

maintenance costs [25]. However, the maintenance costs of other electrical components such as motor/converter are not considered in this research work due to the lack of public domain data. The battery replacement cost $C_{Battery,FC}$ associated with each flight cycle is estimated as Equation (18):

$$C_{Battery,FC} = f_{Battery,FH}(t_{mission}) \cdot t_{mission} \tag{18}$$

Where $f_{Battery,FH}$ is the battery maintenance cost per flight hour which is considered as US$ 205 with the assumption of the battery capital cost as 100 $/kWh [25].

The acquisition cost includes aircraft yearly insurance, interest repayment on capital employed, and the depreciation of capital investment [23]. The annual insurance and interest costs are normally estimated as a percentage of capital investment cost. The depreciation of capital investment is determined by depreciation period and residual value. These costs are initially estimated for a period of one year, and then derived on an hourly basis with the assumed average utilization of flight hours [52]. Then, the acquisition cost per flight cycle is calculated based on mission block time. In this research work, the acquisition cost of both conventional aircraft and its electrified propulsion derivative are considered to be equal.

The capital investment cost is given as equation (19):

$$\begin{aligned} C_{Capital\ Investment} &= C_{Aircraft} + C_{Aircraft,spares} + C_{Propulsion} + C_{Propulsion,spares} \\ C_{Propulsion} &= C_{Engines} + C_{Battery} + C_{Motor/Inverter} \end{aligned} \tag{19}$$

Where $C_{Capital\ Investment}$ is the capital investment cost, $C_{Aircraft}$ is the acquisition price of the aircraft, $C_{Propulsion}$ is the acquisition price of the propulsion, $C_{Aircraft,spares}$ is the cost of aircraft spares as a percentage of aircraft cost, $C_{Propulsion,spares}$ is the cost of propulsion spares as a percentage of propulsion cost, $C_{Engines}$ is the acquisition price of the engines, $C_{Battery}$ is the acquisition price of battery, $C_{Motor/Inverter}$ is the acquisition price of motor and inverter.

Thus, the depreciation cost of aircraft per year $C_{Depreciation,PY}$ can be calculated by assuming a straight-line depreciation method [54] as equation (20):

$$C_{Depreciation,PY} = \frac{C_{Capital\ Investment}(1 - residual_{\%})}{Y_{Life}} \tag{20}$$

Where Y_{Life} is the aircraft operational life, $residual_{\%}$ is the residual value of the aircraft due to the depreciation at the end of operational life.

The annual insurance cost $C_{Insurance,PY}$ and interest cost $C_{Interest,PY}$ are normally estimated as a percentage of capital investment cost as equation (21):

$$\begin{aligned} C_{Interest,PY} &= C_{Capital\ Investment} \cdot Interest_{\%} \\ C_{Insurance,PY} &= C_{Capital\ Investment} \cdot Insurance_{\%} \end{aligned} \tag{21}$$

Thus, the acquisition cost per flight hour $C_{Acquisition,FH}$ can be calculated based on annual utilization in terms of flight hours $h_{annul\ utilization}$. The acquisition cost per flight cycle $C_{Acquisition,FC}$ is calculated based on the mission block time as equation (22):

$$\begin{aligned} C_{Acquisition,FH} &= \frac{C_{Interest,PY} + C_{Insurance,PY} + C_{Depreciation,PY}}{h_{annul\ utilization}} \\ C_{Acquisition,FC} &= C_{Acquisition,FH} \cdot t_{mission} \end{aligned} \tag{22}$$

The parameters of acquisition cost are summarised in Table 4 [25, 53].

The breakeven electricity price is derived as a function of associated DOC components to baseline conventional aircraft [54] in equation (23):

$$\begin{aligned} C_{Breakeven,electricity} &= \frac{C_{fuel} \cdot \triangle W_f + \sum C_{i,Baseline} - \sum C_{i,HEA}}{E_{bat,discharged}} \\ \Delta W_f &= W_{f,Baseline} - W_{f,HEA} \end{aligned} \tag{23}$$

Where $C_{Breakeven,electricity}$ is the breakeven electricity price, C_i represents the associated components of DOC (insurance, interests, maintenance, acquisition, emissions cost etc.), ΔW_f represents the reduction in block fuel burn.

4. Results and discussions

4.1. Flight data analysis and clustering

The GMM fit is tuned by adjusting the number of components and the covariance matrix structure, including spherical, tied, full or diagonal covariance. Normally, Bayesian information criterion (BIC) is selected as the assessment criteria to evaluate the model regression performance [55]. The error of flight route data clustering can be improved by increasing the number of components. However, no significant improvement on BIC scores can be observed when the number of components is over 4. For the purpose of computational efficiency and accuracy, the model is selected with 5 components and diagonal covariance in this case, as shown in Fig. 8.

The results of historical flight operational data clustering and the probability density using GMM are shown in Fig. 9 and Table 5.

4.2. Robust optimal design of hybrid electric aircraft

Fig. 10 presents the sampling results for design variables of P_{Design_Motor} and $E_{Design\_Battery}$ using optimal OA-based Latin hypercubes.

Based on the inputs of flight mission clusters and sampled design variables, HEA mission analysis is simulated which considers fully coupled propulsion-aerodynamic effects. Based on the HEA mission simulation results, the fuel economy surrogate models and their error distributions for each cluster are established using SVMs algorithm, as shown from Fig. 11 to Fig. 15. As indicated in Figs. 11–15, the optimal design point for block fuel burn varies with flight mission profile. Particularly for the scenario of DC3, several sampling points of motor power capacity and battery energy capacity are not feasible to achieve

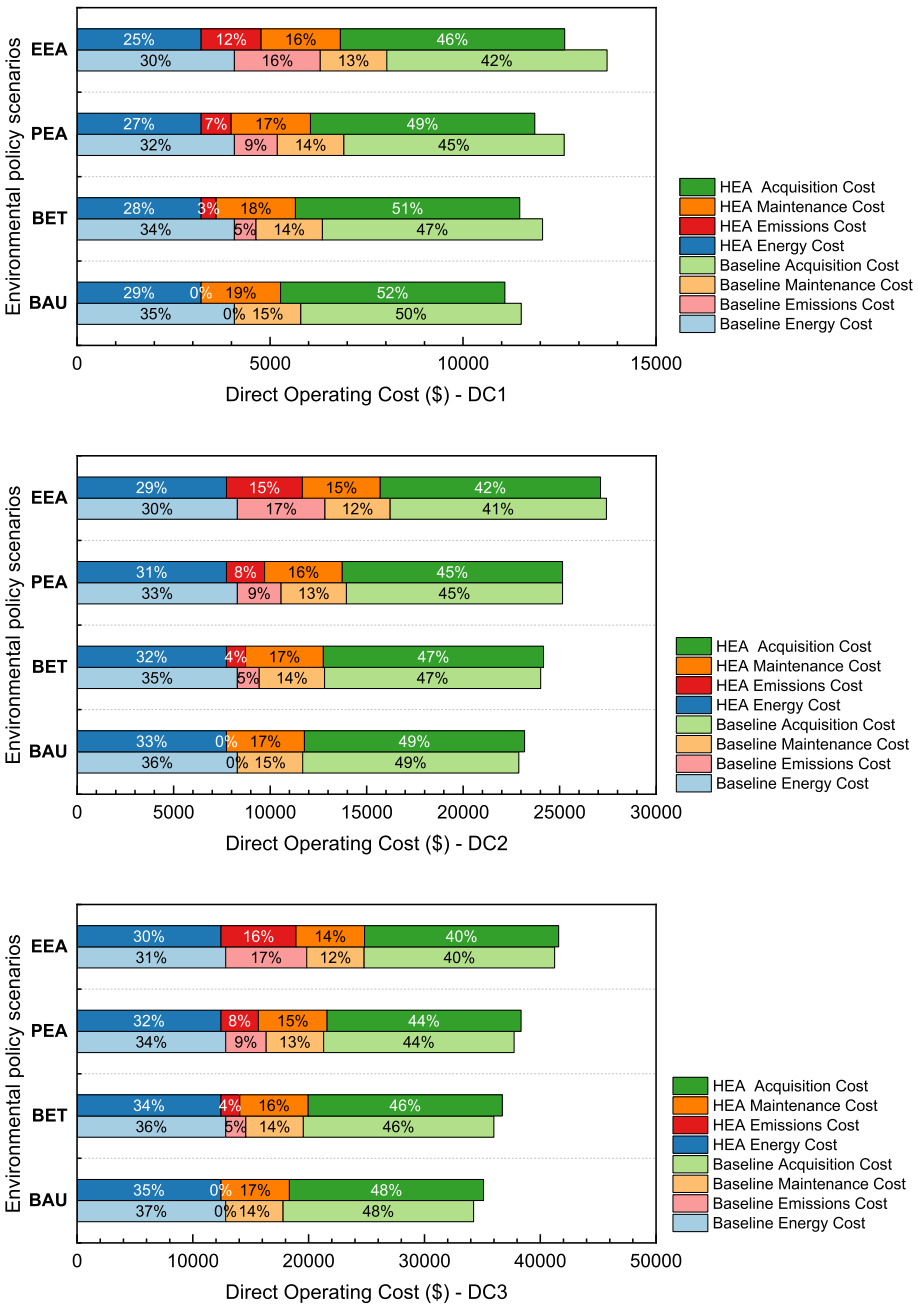

Fig. 19. Direct Operating cost for baseline and HEA optimal design.

because of the constriant violation.

The regression of fuel economy surrogate model is validated using root mean square error (RMSE), coefficient of determination (R-Squared), and mean absolute error (MAE)in Table 6. The results indicate that the proposed model can accurately estimate the HEA fuel economy performance. The error of the regression can be further improved by increasing the size of sampling points. However, the further raise in sampling size will result in the largely increased computational burden.

As shown in Fig. 16, multi-mission fuel economy surrogate model is established by integrating individual block fuel burn surrogate model and the corresponding probability density. Then, the HEA optimal design is obtained which considers the historical flight route data and subsequently reflects the variability in HEA operations.

As shown in Fig. 17, the proposed multi-mission optimal design is able to reduce the block fuel burn by 37.76%, 16.81%, 10.39%, 26.49%, and 14.71% respectively for the representative mission profiles.

4.3. Results of environmental analysis

Based on the emissions prediction model, the direct and indirect emissions including CO_2 and NOx emissions are predicted for individual flight mission profile respectively. As shown in Fig. 18, the results of total CO_2 emissions can be effectively reduced by 7.35%–30.25%, where the indirect CO_2 emissions can be potentially reduced further by using low-carbon energy sources in aircraft charging. In terms of NOx emissions, the potential benefits of 43.88%, 27.08%, 5.23%, 14.01% and 6.75% emissions reduction can be achieved due to the reduced fuel flow rate and more efficient gas turbine operations.

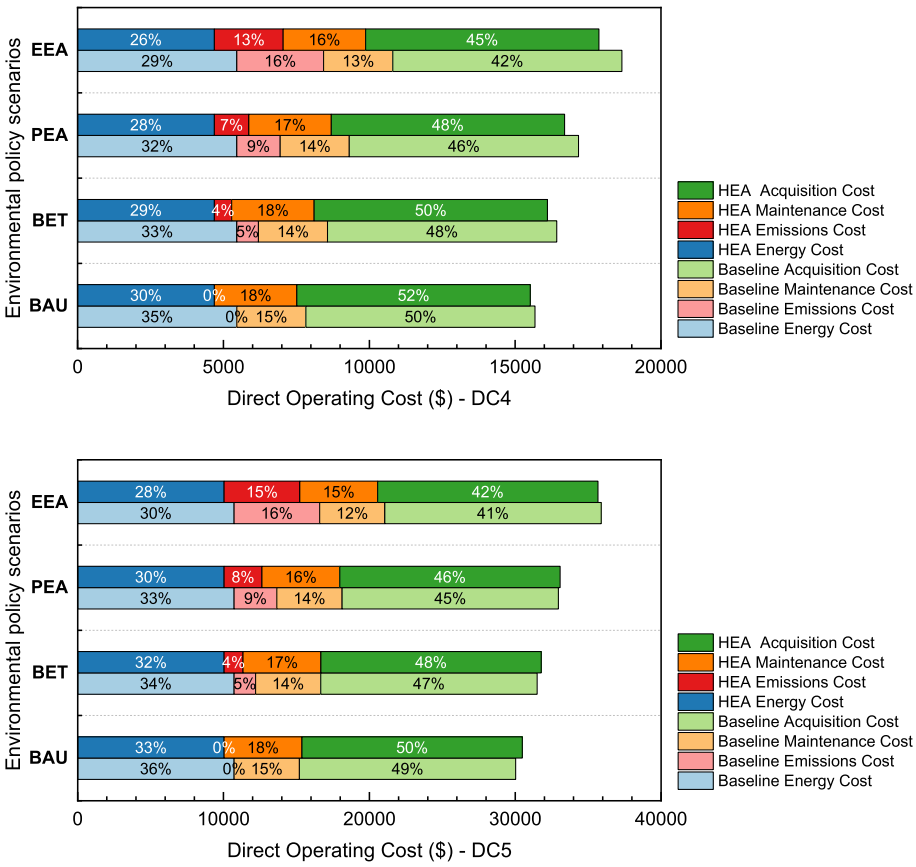

Fig. 19. (*continued*).

4.4. Results of economic analysis

Economic analysis is performed for the baseline conventional aircraft and its electrified propulsion derivatives at integrated aircraft/mission level. Herein, the flight route clusters of DC1to DC5 are used in the case studies for economic viability assessment.

The results of DOC under potential environment regulatory policy scenarios are compared in Fig. 19 for baseline conventional aircraft and HEA optimal design respectively. For DC1, under current price of fuel and electricity, the DOC can be reduced by 3.67%, 4.90%, 6.02%, and 7.98% respectively for environmental policy scenarios of BAU, BET, PEA, and EEA. However, for DC2, no significant benefits of DOC can be observed for BAU and BET due to the less effective (18.61% and 13.27%) block fuel burn reduction and carbon emissions reduction, thus the reduction of HEA energy cost and emissions cost cannot compensate for the induced acquisition and maintenance costs of electric powertrain. However, in the environmental policy scenario of EEA, the DOC can be slightly reduced by 1.11% for DC2. Furthermore, in DC3, the penalties on DOC can be observed, where the DOCs are even increased by 2.52%, 2.03%, 1.60%, and 0.84% for BAU, BET, PEA, and EEA respectively since the block fuel burn and CO_2 emissions only slightly reduce by 10.81% and 7.35%. In DC4, the block fuel burn and carbon emissions are significantly reduced with propulsion electrification, thus DOC reduction can be achieved from 1.04% to 4.20%. For DC5, the slightly increased DOC can be observed in BAU, BET, and PEA from 1.5% to 0.36%, and only a slight DOC reduction of 0.61% can be obtained with relatively high carbon tax of 200 $/Metric Ton.

In summary, under the current price of fuel and electricity, the potential benefits of propulsion electrification on DOC reductions can be observed in short-haul flights (e.g., DC1, DC4), where the block fuel burn and CO_2 emissions can be significantly reduced. For long flight route clusters (e.g., DC2, DC3 and DC5), exceptional environmental awareness with relatively high carbon tax are required for aircraft propulsion electrification to achieve DOC reductions. It should be noted that these case studies are calculated under the assumptions that the maintenance cost for airframe and engines are equal in baseline conventional aircraft and its electrified propulsion derivatives. The impact of electrification on engine operational life is not considered. However, electrical power on-take in HEA can effectively reduce turbine entry temperature compared to the baseline conventional engine, hence positively affecting gas turbine operational life [8]. Besides, the propulsion system is currently modelled by retrofitting the gas turbine with electrical power on-take without modifying the engine cycle. The engine cycle re-design by considering hybridization can further improve the benefits of fuel economy and emissions reduction. Thus, the further DOC reduction can be potentially achieved more than expected in this research work.

In the previous discussions, the quantified benefits of DOC reductions have been demonstrated. However, with advances in battery, electric machine and converter technologies and their potential deployment in production scale, the capital and maintenance costs of electric powertrain are expected to reduce significantly. The associated cost estimation of EAP is highly uncertain due to the uncertainties in the development and deployment of these technologies. In order to investigate the uncertainty effects of the maintenance and acquisition costs on DOC, a sensitivity analysis is presented under potential environmental regulatory policy scenarios of BAU, BET, PEA, and EEA respectively in Fig. 20.

As shown in Fig. 20, for the flight route cluster of DC1, based on the current price of fuel (1157.10 $/Metric Ton) and electricity (10.55 Cents/kWh), the potential cost benefits can be observed in all the environmental policy scenarios. At the datum points, the advantages of DOC reduction can be observed from −7.49% in BAU to −11.17% in EEA. The potential benefits on DOC reduction is primarily provided by

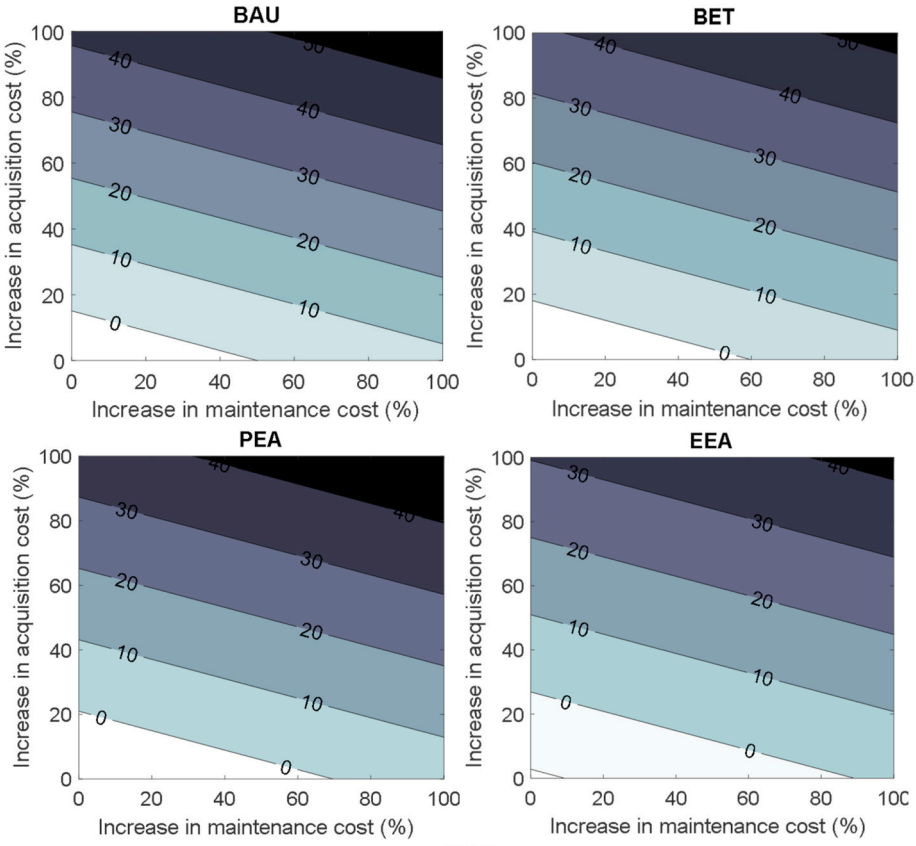

a. DC1

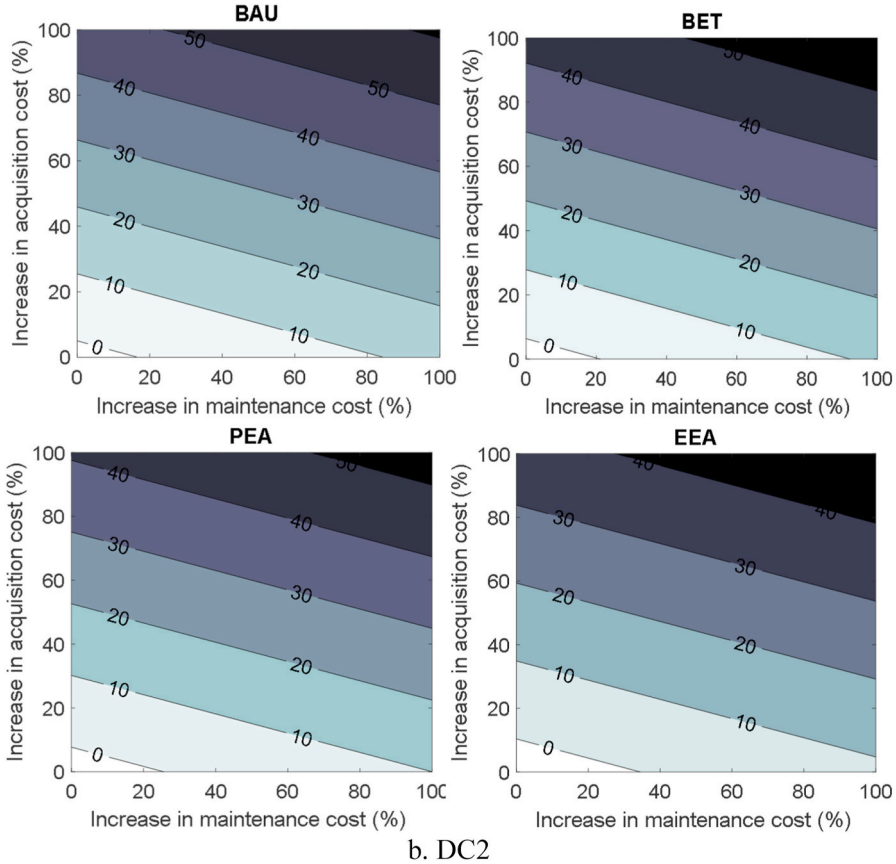

b. DC2

Fig. 20. Direct Operating cost for baseline and HEA optimal design.

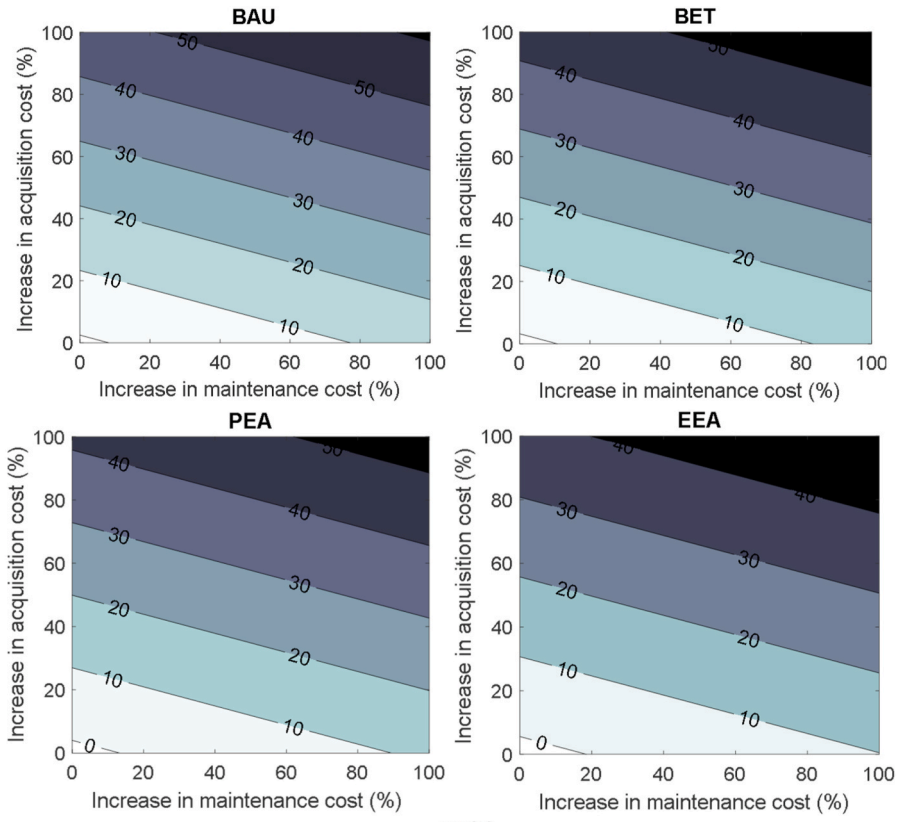

c. DC3

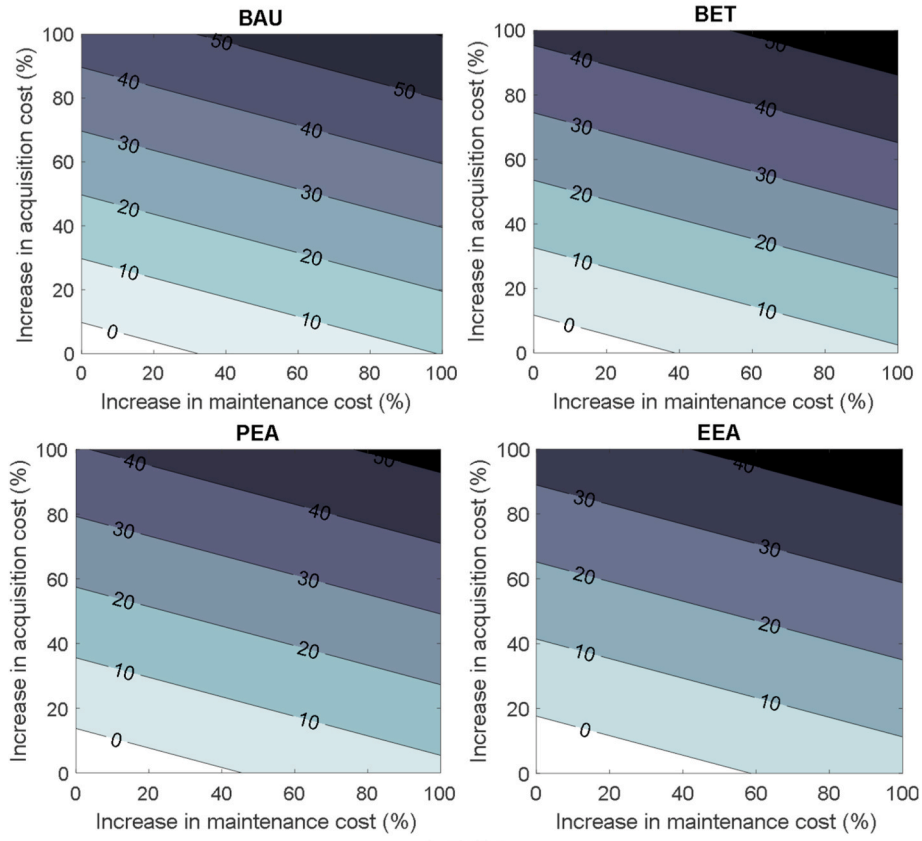

d. DC4

Fig. 20. (*continued*).

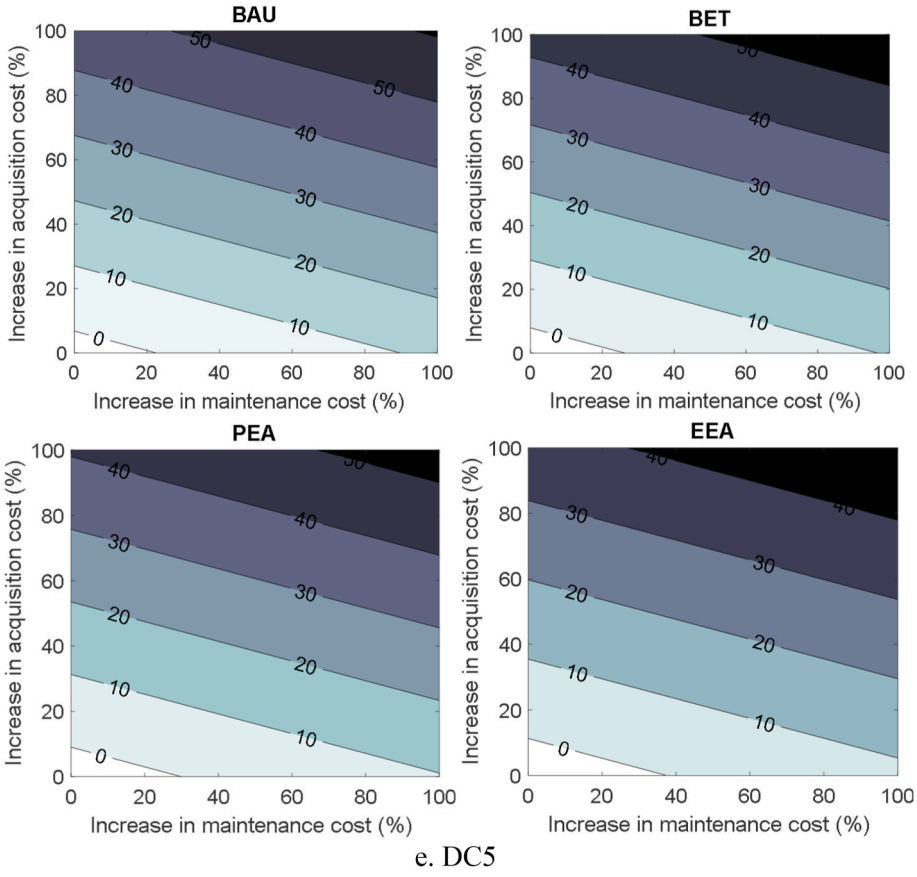

e. DC5

Fig. 20. (*continued*).

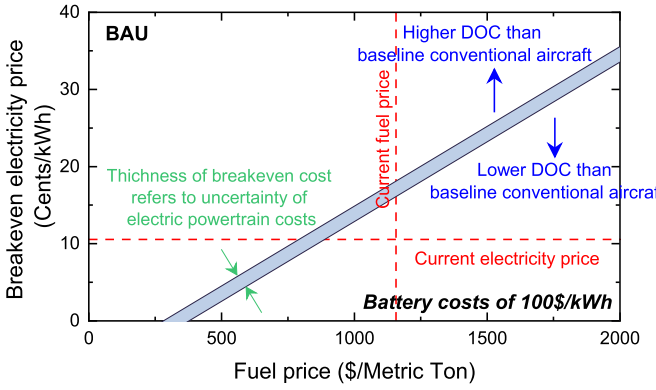

Fig. 21. The breakeven electricity prices versus fuel price example.

the block fuel burn reduction and carbon emissions reductions. Thus, the increasing carbon tax from BAU to EEA scenarios shows an enhanced effect on the potential benefits of DOC reduction. The relative improvement in DOC is degraded accordingly and eventually reduced to 0 in respond to the increases in acquisition and maintenance costs. The similar results can be observed for DC4, the DOC under environmental policy scenarios from BAU to EEA can be reduced from 4.88% to 7.44% at datum points.

However, no promising benefits (less than 1%–2%) of DOC reduction can be obtained even at datum points for DC2, DC3 and DC5 of long-haul flights. The sensitivity analysis shows the energy and emissions cost savings are not capable of compensating the greatly raised capital investment and maintenance costs of electric powertrain.

Fig. 21 presents an example of cost-effectiveness analysis on the breakeven electricity price for flight route cluster of DC1 under the environmental policy scenario of BAU, associated with the battery capital cost of 100$/kWh and the maintenance cost of 205 $/FH. As illustrated, above the breakeven cost line, the DOC of HEA is higher than baseline conventional aircraft, and vice versa. Particularly, the thickness of the breakeven cost line reflects the uncertainty of electric powertrain costs since the maintenance costs of motor/converter are not considered due to the lack of public domain data. For current price of fuel and electricity in BAU, the promising benefits of DOC reduction can be observed for HEA optimal design in short-haul flights.

The breakeven electricity prices under environmental regulatory policy scenarios are shown in Fig. 22. In this case study, the battery capital investment cost is assumed as 100 $/kWh and 200 $/kWh respectively, which corresponds to the battery replacement and maintenance cost of 205 $/FH and 410 $/FH [25].

For DC1 in the environmental policy scenario of BAU, considering the current electricity price of 10.55 Cents/kWh, fuel prices are required to be above 839.74 $/Metric ton and 1169.3 $/Metric ton respectively to achieve cost effectiveness. For the scenarios of BET, PEA and EEA, the required breakeven fuel prices are further reduced due to the relatively higher carbon tax and emissions costs. The breakeven fuel/electricity prices are dependent on battery capital/maintenance costs. By assuming higher battery capital/maintenance cost, the breakeven electricity price will be lower, because the cost of electricity has to be reduced to compensate for the higher associated costs of electric components.

The case of DC4 for short-haul flights is also effective in DOC reduction. By considering the current electricity price to be 10.55 cents/kWh, the cost-effectiveness of EAP can be obtained if the fuel price is above 1027.05 $/Metric ton, 902.59 $/Metric ton, 778.13 $/Metric ton, and 529.23 $/Metric ton respectively, which correspond to the battery capital cost of 100 $/kWh in four different environmental policy scenarios of BAU, BET, PEA and EEA. If the battery capital cost is doubled to

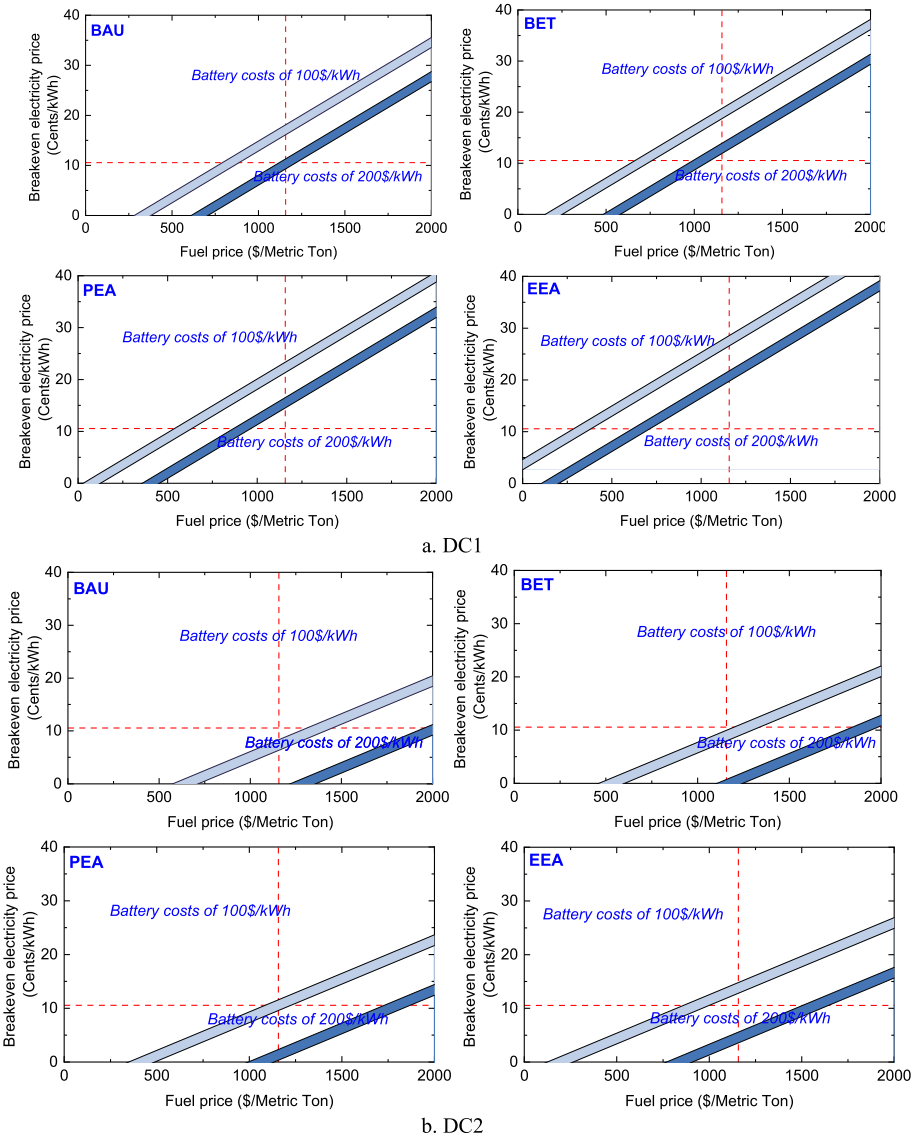

Fig. 22. Breakeven electricity prices for battery capital costs of 100$/kWh and 200$/kWh.

be 200 $/kWh, the fuel price is required to be increased accordingly to the threshold values of 1510.42 $/Metric ton, 1386.07 $/Metric ton, 1261.52 $/Metric ton, and 1012.63 $/Metric ton respectively.

However, the cost-effectiveness is largely dependent on the potential block fuel burn reduction and carbon emissions reduction. For DC2, DC3, and DC5 with long-haul flights, the potential benefits on block fuel burn and emissions are not as effective as short-haul flight clusters of DC1 and DC4. Therefore, the breakeven electricity price is required to be unrealistic low. For example, by assuming the battery capital and maintenance cost to be 200 $/kWh for long-haul flight cluster DC2 under BAU and BET environmental policy scenarios, even the electricity price is set to an extreme case of 0 $/kWh, there is no benefits on DOC reduction can be observed. In DC3, for battery capital cost of 100 $/kWh, the fuel prices need to be above very high threshold values of 1875.91 $/Metric ton, 1768.58 $/Metric ton, 1661.15 $/Metric ton, and 1446.39 $/Metric ton respectively. For DC3, in terms of battery capital cost of 200 $/kWh for all the environmental policy scenarios, none of DOC reduction can be achieved as cost effectiveness if the fuel price is within 2000 $/Metric ton. The similar result occurs in DC5, with the high battery capital cost of 200 $/kWh and associated battery maintenance cost of 410 $/FH, the breakeven electricity prices become unrealistic negative values (below 0 $/kWh) in all the environmental policy scenarios. For the battery capital cost of 200 $/kWh, the DOC reduction can be achieved if the fuel price is increased to 1460.75 $/Metric ton, 1345.09 $/Metric ton, 1229.27 $/Metric ton, and 997.73 $/Metric ton respectively for the environmental policy scenarios of BAU, BET, PEA and EEA.

5. Conclusion

A multi-mission optimal design approach for HEA is proposed to integrate flight operational data into the EAP design procedure, to achieve promising fuel economy benefits over multiple flight missions and conditions. At the first design stage, GMM is used for data clustering, to identify the grouping of flight operational data and obtain a set of representative flight mission profiles. In the DOE stage, OA-based Latin hypercubes method is employed to generate a set of sampling points for the design variables of EAP. Following that, the HEA mission analysis procedure with EMS optimization is simulated to obtain fuel economy for all the sampling points of EAP design variables with the representative flight mission profiles. On this basis, the fuel economy surrogate model is established by using nonlinear SVMs methods. Finally, the

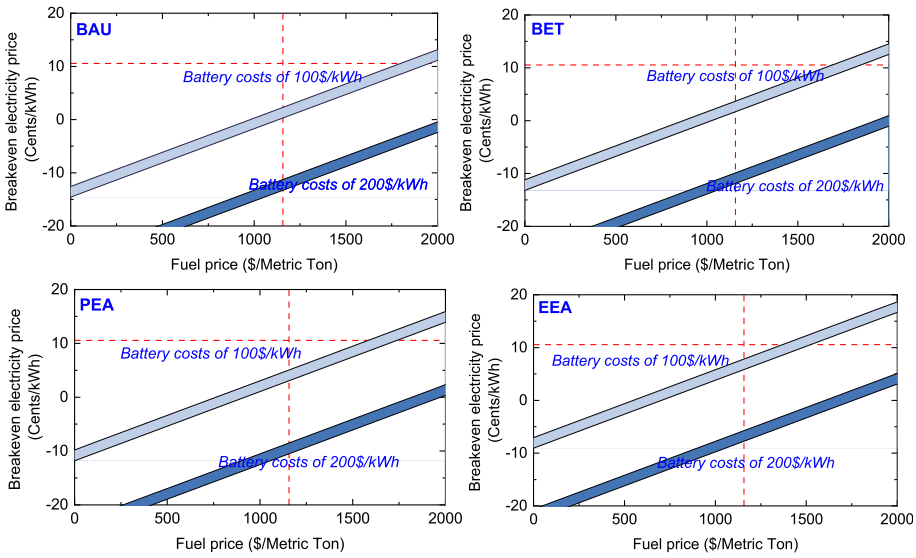

c. DC3

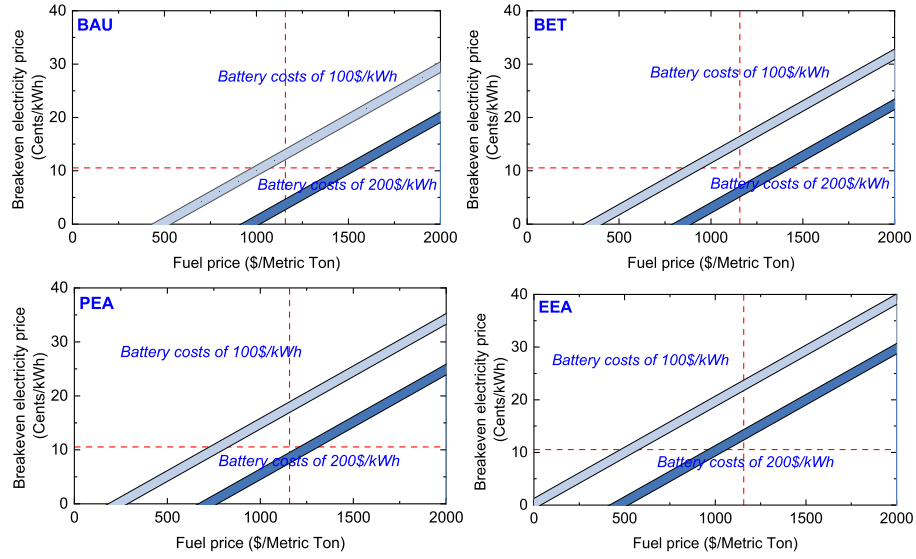

d. DC4

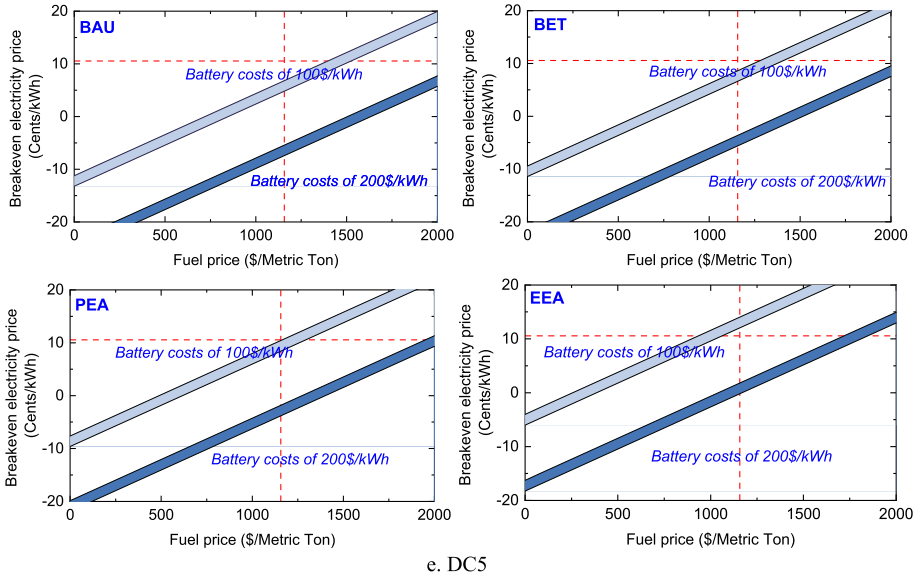

e. DC5

Fig. 22. (*continued*).

optimal design of motor power capacity and battery energy storage capacity are achieved. The surrogate-based optimal design approach can effectively address the optimal design challenges in aircraft propulsion electrification, with complex objective functions evaluations with high computational burdens.

Based on HEA optimal design, environmental and economic assessments are presented for the cost-effectiveness analysis of aircraft propulsion electrification. In particular, on-board direct combustion CO_2 emissions and NOx emissions, and non-direct CO_2 emissions from ground energy infrastructure, are evaluated. On this basis, the economic analysis is presented by using DOC as the most essential assessment criteria. DOC mainly consists of energy cost (fuel and electricity), engine and airframe maintenance cost with battery replacement cost, acquisition cost and emissions cost. A sensitivity analysis of acquisition and maintenance cost to DOC is conducted. Finally, the breakeven electricity prices for potential environmental regulatory policy scenarios are investigated. In conclusion, under the current price of fuel and electricity, the potential benefits of DOC reduction can be observed in short-haul flights, where the block fuel burn and carbon emissions can be significantly reduced. For long-haul flight ranges, more incentivised environmental policy scenarios with high carbon tax, as well as the lower costs of aircraft propulsion electrification technologies are required to achieve cost-effectiveness of aircraft propulsion electrification.

In the future research work, the limitations of this study will be further improved. The EAP is currently modelled by simply retrofitting the gas turbine with electrical power on-take but without modifying the engine. The engine cycle re-design will be further explored which has the potentials to further improve the fuel economy benefits. Also, the differences in engine/airframe maintenance costs between conventional aircraft and HEA are required to be investigated, where the impacts of electrification on gas turbine operational life should be considered.

Credit author statement

Jinning Zhang: Writing – original draft, Methodology, Formal analysis, Software, Investigation, Formal analysis, Validation, **Ioannis Roumeliotis:** Writing – review & editing, Supervision, Investigation, **Xin Zhang:** Writing – review & editing, Supervision, Investigation, **Argyrios Zolotas:** Writing – review & editing, Formal analysis, Supervision

Declaration of competing interest

The authors declare that they have no known competing financial interests or personal relationships that could have appeared to influence the work reported in this paper.

Data availability

Data will be made available on request.

References

[1] Schwab A, Thomas A, Bennett J, Robertson E, Cary S. Electrification of aircraft: challenges, barriers, and potential impacts (No. NREL/TP-6A20-80220). Golden, CO (United States): National Renewable Energy Lab.(NREL); 2021.

[2] Zhang J, Roumeliotis I, Zolotas A. Sustainable aviation electrification: a comprehensive review of electric propulsion system architectures, energy management, and control. Sustainability 2022;14(10):5880.

[3] Guo Z, Zhang J, Zhang R, Zhang X. Aviation-to-Grid flexibility through electric aircraft charging. IEEE Trans Ind Inf 2021.

[4] National Academies of Sciences, Engineering, and Medicine. Commercial aircraft propulsion and energy systems research: reducing global carbon emissions. National Academies Press; 2016.

[5] Brelje BJ, Martins JR. Electric, hybrid, and turboelectric fixed-wing aircraft: a review of concepts, models, and design approaches. Prog Aero Sci 2019;104:1–19.

[6] Viswanathan V, Knapp BM. Potential for electric aircraft. Nat Sustain 2019;2(2):88–9.

[7] Adibhatla S, Ding J, Garg S, Griffith S, Karnofski K, Payne N, Wood B. Propulsion control technology development needs to address NASA aeronautics research mission goals for thrusts 3a and 4. In American Institute of Aeronautics and Astronautics (AIAA) Propulsion and Energy Forum 2018 2018, July. *No. GRC-E-DAA-TN57637)*.

[8] Kang S, Roumeliotis I, Zhang J, Broca O, Pachidis V. Assessment of engine operability and overall performance for parallel hybrid electric propulsion systems for a single-aisle aircraft. J Eng Gas Turbines Power 2022;144(4).

[9] Bocii Liviu Sevastian, Di Noia Luigi Pio, Rizzo Renato. Optimization of the energy storage of series-hybrid propelled aircraft by means of integer differential evolution. Aerospace 2019;6(5):59.

[10] Donateo T, Carlà A, Avanzini G. Fuel consumption of rotorcrafts and potentiality for hybrid electric power systems. Energy Convers Manag 2018;164:429–42.

[11] Sliwinski J, Gardi A, Marino M, Sabatini R. Hybrid-electric propulsion integration in unmanned aircraft. Energy 2017;140:1407–16.

[12] Ang AWX, Gangoli Rao A, Kanakis T, Lammen W. Performance analysis of an electrically assisted propulsion system for a short-range civil aircraft. Proc IME G J Aero Eng 2019;233(4):1490–502.

[13] Decerio DP, Hall DK. Benefits of parallel hybrid electric propulsion for transport aircraft. IEEE Transactions on Transportation Electrification 2022.

[14] Finger DF, de Vries R, Vos R, Braun C, Bil C. Cross-validation of hybrid-electric aircraft sizing methods. J Aircraft 2022:1–19.

[15] Yutko BM. The impact of aircraft design reference mission on fuel efficiency in the air transportation system. Doctoral dissertation, Massachusetts Institute of Technology; 2013.

[16] Gladin, J., Harish, A., & Mavris, D. [Multi-Mission Performance Optimization of a Hybrid-Electric Unmanned Aerial Vehicle]...

[17] Perez R, Behdinan K. Effective multi-mission aircraft conceptual design optimization using a hybrid multi-objective evolutionary method. In 9th American Institute of Aeronautics and Astronautics/International Society of Structural and Multidisciplinary Optimization Symposium on Multidisciplinary Analysis and Optimization 2002:5464.

[18] Cai Y, Rajaram D, Mavris DN. Multi-mission multi-objective optimization in commercial aircraft conceptual design. American Institute of Aeronautics and Astronautics Aviation 2019 Forum; 2019. p. 3577.

[19] Liem R, Kenway G, Martins JR. Multi-point, multi-mission, high-fidelity aerostructural optimization of a long-range aircraft configuration. In: 12th American institute of aeron*autics and astronautics aviation technology, integration, and operations (ATIO) Conference and 14th American Institute of Aeronautics and astronautics/international Society of Structural and multidisciplinary optimization multidisciplinary Analysis and optimization conference*; 2012, September. p. 5706.

[20] Liem RP, Kenway GK, Martins JR. Multi-mission aircraft fuel-burn minimization via multipoint aerostructural optimization. American Institute of Aeronautics and Astronautics Journal 2015;53(1):104–22.

[21] Liem RP, Martins JR, Kenway GK. Expected drag minimization for aerodynamic design optimization based on aircraft operational data. Aero Sci Technol 2017;63:344–62.

[22] Kim D, Druot TY, Liem RP. Data-driven operation-based aircraft design optimization. American Institute of Aeronautics and Astronautics Aviation 2020 Forum; 2020. p. 3156.

[23] Goldberg C, Nalianda D, Sethi V, Pilidis P, Singh R, Kyprianidis K. Assessment of an energy-efficient aircraft concept from a techno-economic perspective. Appl Energy 2018;221:229–38.

[24] Kristjanpoller WD, Concha D. Impact of fuel price fluctuations on airline stock returns. Appl Energy 2016;178:496–504.

[25] –> Schäfer AW, Barrett SR, Doyme K, Dray LM, Gnadt AR, Self R, Torija AJ. Technological, economic and environmental prospects of all-electric aircraft. Nat Energy 2019;4(2):160–6.

[26] Ribeiro J, Afonso F, Ribeiro I, Ferreira B, Policarpo H, Peças P, Lau F. Environmental assessment of hybrid-electric propulsion in conceptual aircraft design. J Clean Prod 2020;247:119477.

[27] Kreimeier M, Stumpf E. Benefit evaluation of hybrid electric propulsion concepts for CS-23 aircraft. Council of European Aerospace Societies (CEAS) Aeronautical Journal 2017;8(4):691–704.

[28] Gnadt AR, Speth RL, Sabnis JS, Barrett SR. Technical and environmental assessment of all-electric 180-passenger commercial aircraft. Prog Aero Sci 2019;105:1–30.

[29] Ribeiro RF, Trapp LG, Lacava P. Economical aspects of aircraft propulsion electrification. In American Institute of Aeronautics and Astronautics Propulsion and Energy 2021 Forum; 2021. p. 3329.

[30] Scholz AE, Trifonov D, Hornung M. Environmental life cycle assessment and operating cost analysis of a conceptual battery hybrid-electric transport aircraft. Council of European Aerospace Societies (CEAS) Aeronautical Journal 2022;13(1):215–35.

[31] Wehrspohn J, Rahn A, Papantoni V, Silberhorn D, Burschyk T, Schröder M, Wende G. A detailed and comparative economic analysis of hybrid-electric aircraft concepts considering environmental assessment factors. In American Institute of Aeronautics and Astronautics AVIATION 2022 Forum; 2022. p. 3882.

[32] Finger DF, Goetten F, Braun C, Bil C. Cost estimation methods for hybrid-electric general aviation aircraft. In: In 2019 asia-pacific international sympo*sium on aerospace technology*. APISAT 2019; 2019, December. p. 265–77.

[33] Moebs N, Eisenhut D, Bergmann D, Strohmayer A. Selecting figures of merit for a hybrid-electric 50-seat regional aircraft. In: In IOP conference series: materials science and engineering, vol. 1024. IOP Publishing; 2021, 012071. No. 1.

[34] Air carrier Statistics (form 41 traffic)- all carriers. Available at: https://www.transtats.bts.gov/databases.asp?Z1qr_VQ=E&Z1qr_Qr5p=N8vn6v10&f7owrp6_VQF=D. [Accessed 19 March 2021].
[35] Boeing 737 airplane characteristics for airport planning. Available at: https://www.boeing.com/commercial/airports/plan_manuals.page. [Accessed 19 March 2021].
[36] He X, Cai D, Shao Y, Bao H, Han J. Laplacian regularized Gaussian mixture model for data clustering. IEEE Trans Knowl Data Eng 2010;23(9):1406–18.
[37] Pernkopf F, Bouchaffra D. Genetic-based EM algorithm for learning Gaussian mixture models. IEEE Trans Pattern Anal Mach Intell 2005;27(8):1344–8.
[38] Zhang J, Roumeliotis I, Zolotas A. Model-based fully coupled propulsion-aerodynamics optimization for hybrid electric aircraft energy management strategy. Energy 2022:123239.
[39] Zhang J, Roumeliotis I, Zolotas A. Nonlinear model predictive control-based optimal energy management for hybrid electric aircraft considering aerodynamics-propulsion coupling effects. IEEE Transactions on Transportation Electrification 2021.
[40] Dever TP, Duffy KP, Provenza AJ, Loyselle PL, Choi BB, Morrison CR, Lowe AM. *Assessment of technologies for noncryogenic hybrid electric propulsion* (No. GRC-E-DAA-TN10454). Available at: https://ntrs.nasa.gov/api/citations/20150000747/downloads/20150000747.pdf; 2015.
[41] Sahoo S, Zhao X, Kyprianidis K. A review of concepts, benefits, and challenges for future electrical propulsion-based aircraft. Aerospace 2020;7(4):44.
[42] Leary S, Bhaskar A, Keane A. Optimal orthogonal-array-based Latin hypercubes. J Appl Stat 2003;30(5):585–98.
[43] Queipo NV, Haftka RT, Shyy W, Goel T, Vaidyanathan R, Tucker PK. Surrogate-based analysis and optimization. Prog Aero Sci 2005;41(1):1–28.
[44] Eldred M, Dunlavy D. Formulations for surrogate-based optimization with data fit, multifidelity, and reduced-order models. In: 11th American institute of aeronautics and astronautics/international Society of Structural and multidisciplinary Optimization multidisciplinary analysis and optimization conference; 2006, September. p. 7117.
[45] Sacks Jerome William J Welch, Mitchell Toby J, Wynn Henry P. Design and analysis of computer experiments. Stat Sci 1989;4(4):409–23.
[46] Greiner D, Galván B, Périaux J, Gauger N, Giannakoglou K, Winter G, editors. Advances in evolutionary and deterministic methods for design, optimization and control in engineering and sciences. Switzerland: Springer International Publishing; 2015.
[47] Huang TM, Kecman V, Kopriva I. Kernel based algorithms for mining huge data sets, vol. 1. Heidelberg: Springer; 2006.
[48] UK carbon intensity API. Available at: https://carbonintensity.org.uk./.
[49] Kyprianidis KG, Nalianda D, Dahlquist E. A NOx emissions correlation for modern RQL combustors. Energy Proc 2015;75:2323–30.
[50] IATA jet fuel price monitor. Available at: https://www.iata.org/en/publications/economics/fuel-monitor/.
[51] EIA average price of electricity to ultimate customers. Available at: https://www.eia.gov/electricity/monthly/epm_table_grapher.php?t=epmt_5_03.
[52] Nalianda DK, Kyprianidis KG, Sethi V, Singh R. Techno-economic viability assessments of greener propulsion technology under potential environmental regulatory policy scenarios. Appl Energy 2015;157:35–50.
[53] Nalianda Karumbaiah D. Impact of environmental taxation policies on civil aviation-a techno-economic environmental risk assessment, *Phd thesis*. Cranfield University; 2012.
[54] Goldberg C. Techno-economic, environment and risk analysis of an aircraft concept with turbo-electric distributed propulsion, *Phd thesis*. Cranfield University; 2017.
[55] Vrieze SI. Model selection and psychological theory: a discussion of the differences between the Akaike information criterion (AIC) and the Bayesian information criterion (BIC). Psychol Methods 2012;17(2):228.